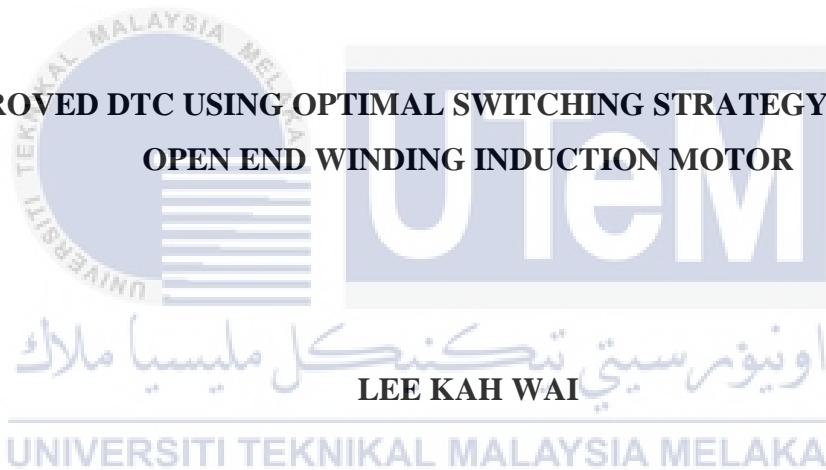




Faculty of Electrical Engineering

**IMPROVED DTC USING OPTIMAL SWITCHING STRATEGY FOR DUAL-
OPEN END WINDING INDUCTION MOTOR**

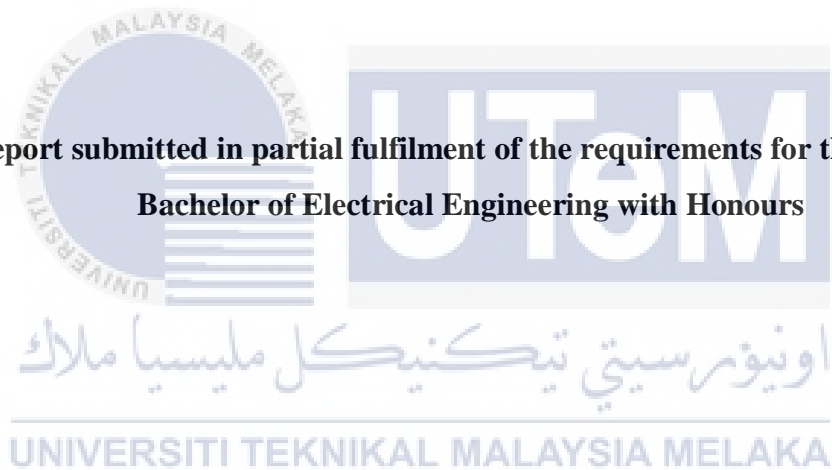


Bachelor of Electrical Engineering with Honours

**IMPROVED DTC USING OPTIMAL SWITCHING STRATEGY FOR DUAL-
OPEN END WINDING INDUCTION MOTOR**

LEE KAH WAI

**A report submitted in partial fulfilment of the requirements for the degree of
Bachelor of Electrical Engineering with Honours**



Faculty of Electrical Engineering

UNIVERSITI TEKNIKAL MALAYSIA MELAKA

2019

DECLARATION

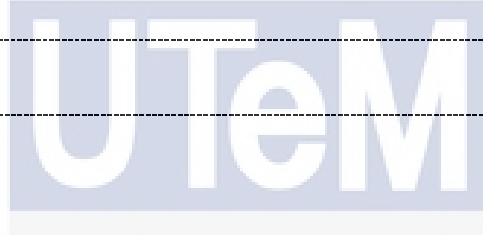
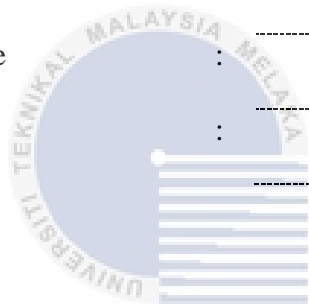
I declare that this thesis entitled “Improved DTC using Optimal Switching Strategy for Dual-Open End Winding Induction Motor is the result of my own research except as cited in the references. The thesis has not been accepted for any degree and is not concurrently submitted in candidature of any other degree.

Signature :

Name :

Date :

LEE KAH WAI



اونيورسيتي تيكنيكل مليسيا ملاك

UNIVERSITI TEKNIKAL MALAYSIA MELAKA

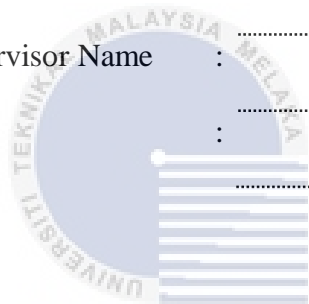
APPROVAL

I hereby declare that I have checked this report entitled “Improved DTC using Optimal Switching Strategy for Dual-Open End Winding Induction Motor” and in my opinion, this thesis it complies the partial fulfillment for awarding the award of the degree of Bachelor of Electrical Engineering with Honours

Signature :

Supervisor Name :

Date :



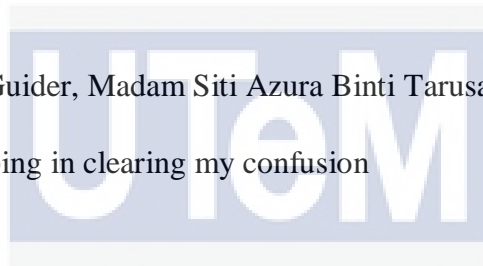
اونيورسيتي تيكنيكل مليسيا ملاك

UNIVERSITI TEKNIKAL MALAYSIA MELAKA

DEDICATIONS

To my beloved mother and father
For giving the support in all perspective

To my respectful supervisor, Dr. Auzani Bin Jidin
For giving the endless support, guidance and teaching



To my respectful Guider, Madam Siti Azura Binti Tarusan
For helping in clearing my confusion

اونيور سیتی تیکي کل ملیسيا ملاک
My friends

For their moral support and encouragement through my journey of education

UNIVERSITI TEKNIKAL MALAYSIA MELAKA

ACKNOWLEDGEMENTS

First of all, I would like to thank University Technical Malaysia Melaka for giving this opportunity to me to complete my studies and also this research. Besides, not to forget, I would like to express my special thanks of gratitude to my supervisor Dr Auzani Bin Jidin for the help, advise, recommendation and guidance in order to help me achieve the objective of this thesis. The supervision and support that he gave truly help in the progression and smoothness of this research. Without mentioning, all the other lecturers involved in this research either directly or indirectly, especially to the entire lecture who have taught me, thank you for the time for the lessons that have been taught which enlightened me.

My sincere thanks to all my friends in the one same guidance under Dr Auzani Bin Jidin, who willing to lend me their hands and supports when I was confused. A person who gave me advise and helps all the time when my supervisor was busy, Madam Siti Azura Binti Ahmad Tarusan.

In the end, not to forget the one and only one who give me all their support in the journey of my study, my parents. Their support either in mental or financial is a great help for me to strengthen my will in continue this tough journey.

ABSTRACT

Direct Torque Control (DTC) of induction machine has received wide acceptance in many adjustable speed drive applications due to its simplicity and high-performance torque control. However, the DTC using conventional design poses two major problems such as high switching frequency and larger torque ripple. These problems are due to inappropriate voltage vectors which are selected among a limited number of voltage vectors available. The proposed research aims to formulate an optimal switching strategy for dual-open end winding induction motor. By using dual inverters, it provides greater number of voltage vectors which can offer more options to select the most appropriate voltage vectors. By selecting the suitable voltage vectors, it allowed the motor to produce minimum torque slope but enough to reach the required demand. To achieve this result, the proposed method does not require speed information, PI controller, frame transformation, space vector modulator, reference voltage estimator and machine parameters. The improvements obtained are minimizing the switching frequency with reducing the losses and torque ripple reduction.

ABSTRAK

Kawalan dayakilas langsung (DTC) untuk motor aruhan telah mendapatkan penerimaan yang luas dalam kebanyakan aplikasi pemacu pelarasan laju atas sebab reka bentuk ia ringkas dan mempunyai prestasi yang agak tinggi. Walau bagaimanapun, DTC yang menggunakan reka betuk yang biasa menimbulkan dua masalah, iaitu riak dayakilas yang besar dan frekuensi pensuisan yang tinggi. Masalah-masalah tersebut ditimbulkan kerana ketidak sesuaian vektor voltan terpilih antara vektor voltan yang terhad. Kajian yang dicadangkan bertujuan untuk memformulasi sebuah strategi pensuisan yang optimal bagi dual-open end winding motor aruhan dengan memakai dua inverter. Dwi inverter ini akan memberikan lebih banyak pilihan dalam vektor voltan dan mendapatkan vektor voltan yang sesuai untuk situasi motor yang berbeza. Dengan memilih vektor voltan yang sesuai, ia dibenarkan motor untuk menghasilkan cerun minimum tork tapi cukup untuk mencapai permintaan diperlukan. Untuk mencapai keputusan ini, kaedah yang dicadangkan memerlukan kelajuan maklumat, PI pengawal, rangka transformasi, space vektor modulator, rujukan voltan estimator dan parameter mesin. Penambahbaikan yang terdapat daripada kajian yang dicadangkan adalah dapat meminimumkan frekuensi pensuisan yang dijangka akan mengurangkan kehilangan kuasa dan pengurangan riak bagi dayakilas.

TABLE OF CONTENTS

	PAGE
DECLARATION	
APPROVAL	
DEDICATIONS	
ACKNOWLEDGEMENTS	i
ABSTRACT	ii
ABSTRAK	iii
TABLE OF CONTENTS	iv
LIST OF TABLES	vi
LIST OF FIGURES	vii
LIST OF SYMBOLS AND ABBREVIATIONS	xi
LIST OF APPENDICES	xiv
CHAPTER 1 INTRODUCTION	1
1.1 Background	1
1.2 Problem Statement	3
1.3 Objective of Research	4
1.4 Scope of Work	4
1.5 Research Methodology	4
1.6 Thesis Contribution	5
1.7 Thesis Outline	5
CHAPTER 2 LITERATURE REVIEW	6
2.1 Introduction	6
2.2 Direct Torque Control of Induction Machine	6
2.2.1 Voltage Source Inverter (VSI)	7
2.2.2 Stator Flux and Torque Estimator	8
2.2.3 Look-up Table	10
2.3 Principle of Direct Torque Control	11
2.3.1 Principle of Flux Control	11
2.3.2 Principle of Torque Control	13
2.4 Major Problem of Direct Torque Control	15
2.5 Performance Improvements of Direct Torque Control	15
2.5.1 Space Vector Modulation (SVM)	15
2.5.2 Carried Based Modulation	20

CHAPTER 3	METHODOLOGY	24
3.1	Introduction	24
3.2	Mathematical Modelling of an Induction Machine	24
3.3	Dual Voltage Source Inverter	28
3.4	Proposed Optimal Switching Strategy	30
	3.4.1 Principle of Torque Control based on Load Angle, δ_{sr}	30
3.5	Definition of Flux Sectors for Selecting Optimal Voltage Vectors	33
3.6	Look-up Table for Selecting Optimal Voltage Vector	34
3.7	Proposed Control Structure	36
CHAPTER 4	RESULTS AND DISCUSSIONS	38
4.1	Introduction	38
4.2	Torque Ripple Reduction and Switching Frequency Reduction	38
4.3	Reduction of Torque Ripple and Switching Frequency for a Torque Dynamic Control	46
CHAPTER 5	CONCLUSION AND RECOMMENDATIONS	60
5.1	Conclusion	60
5.2	Recommandation	61
REFERENCES		62
APPENDIX A		67
A.1	Sector Detection Block Coding	67
A.2	Look-up Table Coding	69
A.3	Induction Motor Simulation Block Parameters	77
APPENDIX B		78
B.1	Induction Motor Simulation Block	78
B.2	Dual-Voltage Source Inverter Simulation Block	80
B.3	Torque and Flux Estimator Simulation Block	81

LIST OF TABLES

TABLE	TITLE	PAGE
1	LOOK-UP TABLE	10
2	LOOK-UP TABLE FOR SELECTION OPTIMAL VOLTAGE VECTORS IN DUAL-INVERTERS	35



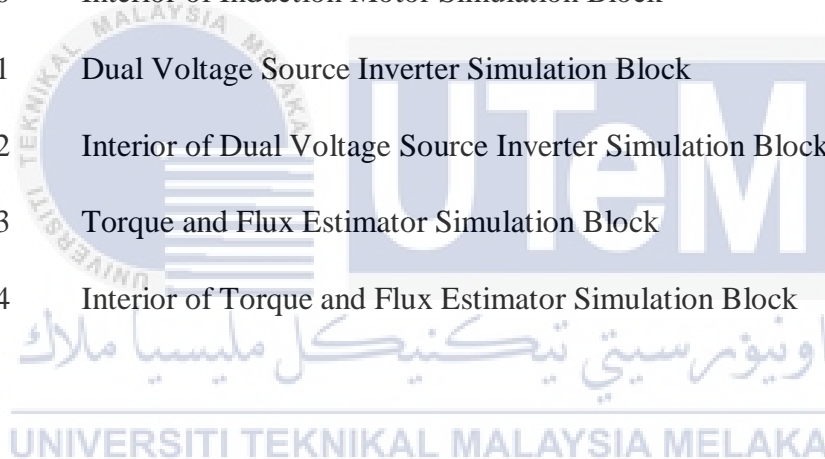
LIST OF FIGURES

FIGURE	TITLE	PAGE
1	FOC and DTC structure	2
2	Structure of DTC of Induction Machine	7
3	Voltage Source Inverter	7
4	Voltage Space Vectors with Corresponded Switching State	8
5	Motion of Stator Flux Vector	11
6	(a) Possible voltage vector for each section, (b) relation between bands and flux error status	12
7	(a) Relation between stator flux and rotor flux and torque, (b) Relation between bands and torque error status	14
8	DTC-SVM structure	16
9	Reference of Space Voltage Vector based on (2.12)	18
10	Generation of Switching of Vectors and its Effect on Torque Variations	19
11	DTC with Dithering Signals Structure	20
12	DTC with Constant Switching Frequency Torque Controller	21
13	Significant Reduction of Torque Ripple with Application of Higher Constant Switching Frequency (a) at Low Carrier Frequency (b) at High Carrier Frequency	22
14	Dual Voltage Source Inverter configuration with Open-End Winding	28
15	Dual Voltage Source Inverter Schematic (Inverter 1)	30
16	Relation between selection of vector and torque and flux status	33

17	Flux sector and suitable Voltage Vector for (a) Long/Short (b) Medium	34
18	Proposed Control Structure of DTC	37
19	Speed of the motor 92rad/s (a) general view (b) Zoomed version	39
20	Waveforms of Torque (T_e), Phase Currents (i_a , i_b , i_c) and Phase Voltage with non-optimized and optimized switching at Low-Speed Operation. (a) General view (b) the zoom-in version	41
21	Speed of the motor 123 rad/s (a) general view (b) Zoomed version	42
22	Waveforms of Torque (T_e), Phase Currents (i_a , i_b , i_c) and Phase Voltage with non-optimized and optimized switching at Medium-Speed Operation. (a) General view (b) the zoom-in version	43
23	Speed of the motor 140rad/s (a) general view (b) Zoomed version	44
24	Waveforms of Torque (T_e), Phase Currents (i_a , i_b , i_c) and Phase Voltage with non-optimized and optimized switching at High-Speed Operation. (a) General view (b) the zoom-in version	45
25	Waveform of Torque, Phase Voltage and Phase current for a Step Change of Reference Torque in DTC with Non-Optimized Switching Strategy at Low-Speed Operation (a) General View (b) Zoom-in Version	47
26	Waveform of Torque, Phase Voltage and Phase current for a Step Change of Reference Torque in DTC with Non-Optimized Switching Strategy at Medium-Speed Operation (a) General View (b) Zoom-in Version	48

27	Waveform of Torque, Phase Voltage and Phase current for a Step Change of Reference Torque in DTC with Non-Optimized Switching Strategy at High-Speed Operation (a) General View (b) Zoom-in Version	49
28	Waveform of Torque, Phase Voltage and Phase current for a Step Change of Reference Torque in DTC with Optimized Switching Strategy at Low-Speed Operation (a) General View (b) Zoom-in Version	50
29	Waveform of Torque, Phase Voltage and Phase current for a Step Change of Reference Torque in DTC with Optimized Switching Strategy at Medium-Speed Operation (a) General View (b) Zoom-in Version	51
30	Waveform of Torque, Phase Voltage and Phase current for a Step Change of Reference Torque in DTC with Optimized Switching Strategy at High-Speed Operation (a) General View (b) Zoom-in Version	52
31	Waveform of Torque, Phase Voltage and Phase current for a Step Reduction of Reference Torque in DTC with Non-Optimized Switching Strategy at Low-Speed Operation (a) General View (b) Zoom-in Version	54
32	Waveform of Torque, Phase Voltage and Phase current for a Step Reduction of Reference Torque in DTC with Non-Optimized Switching Strategy at Medium-Speed Operation (a) General View (b) Zoom-in Version	55
33	Waveform of Torque, Phase Voltage and Phase current for a Step Reduction of Reference Torque in DTC with Non-Optimized Switching Strategy at High-Speed Operation (a) General View (b) Zoom-in Version	56
34	Waveform of Torque, Phase Voltage and Phase current for a Step Reduction of Reference Torque in DTC with Optimized Switching Strategy at Low-Speed Operation (a) General View (b) Zoom-in Version	57

35	Waveform of Torque, Phase Voltage and Phase current for a Step Reduction of Reference Torque in DTC with Optimized Switching Strategy at Medium-Speed Operation (a) General View (b) Zoom-in Version	58
36	Waveform of Torque, Phase Voltage and Phase current for a Step Reduction of Reference Torque in DTC with Optimized Switching Strategy at High-Speed Operation (a) General View (b) Zoom-in Version	59
37	Sector Detection Simulation Block	59
38	Look-up Table Simulation Block	69
39	Induction Motor Simulation Block	78
40	Interior of Induction Motor Simulation Block	79
41	Dual Voltage Source Inverter Simulation Block	80
42	Interior of Dual Voltage Source Inverter Simulation Block	80
43	Torque and Flux Estimator Simulation Block	81
44	Interior of Torque and Flux Estimator Simulation Block	81



LIST OF SYMBOLS AND ABBREVIATIONS

d, q	Direct and quadrature of the stationary reference frame
d^r, q^r	Real and imaginary of the rotor
i_s, i_r	Stator and rotor current space vector in stationary reference frame
R_s, R_r	Stator and rotor resistance
L_s	Stator self-inductance
L_r	Rotor self-inductance
L_m	Mutual inductance
$\bar{\varphi}_s, \bar{\varphi}_r$	Stator and rotor flux linkage space vector in reference frame
i_{rd}, i_{rq}	d and q components of the rotor current in stationary reference frame
i_{sd}, i_{sq}	d and q components of the stator current in stationary reference frame
v_{sd}, v_{sq}	d and q axis of the stator voltage in stationary reference frame
$\varphi_{sd}, \varphi_{sq}$	d and q components of the stator flux in stationary reference frame
\bar{v}_s	Voltage vector
n	Number of phase
i_a, i_b, i_c	Phase current of a, b, c
L	Self-inductance
T_e	Electromagnetic torque
T_e^*	Reference torque
ϵ_T	Output torque error
σ_T	Output torque status

θ_r	Angle with respect to rotor axis
θ_s	Angle with respect to stator axis
δ_{sr}	Different angle between stator flux linkage and rotor flux linkage
V_{DC}	DC link voltage
S_a^+, S_b^+, S_c^+	Switching states of IGBTs
P	Number of pole pair
θ_{sec}	Angle of sector definition
ω_r	Rotor electrical speed in rad/s
ϵ_φ	Output flux error
φ_s^*	Reference of flux
φ_s	Flux estimate
σ_φ	Output flux status
σ	Total flux leakage factor
<i>DTC</i>	Direct Torque Control
<i>IM</i>	Induction Motor
<i>VSI</i>	Voltage Source Inverter
<i>FOC</i>	Field Oriented Control
<i>DT</i>	Sampling period
<i>AC</i>	Alternating Current
<i>DC</i>	Direct Current
<i>SVM</i>	Space Vector Modulator
<i>UB</i>	Upper Band
<i>LB</i>	Lower Band
<i>IGBT</i>	Insulated Gate Bipolar Transistor

i_{sq}^e, i_{sd}^e	Current from the excitation frame
<i>CSFTC</i>	Constant Switching Frequency Torque Controller
<i>PI</i>	Proportional Integral
\bar{i}_s	Current vector



LIST OF APPENDICES

APPENDIX	TITLE	PAGE
A	MATLAB SIMULATION BLOCK CODING	78
B	MATLAB SIMULATION BLOCK	67



CHAPTER 1

INTRODUCTION

1.1 Research Background

Direct torque control (DTC) and Field Oriented Control (FOC) were introduced by Takahashi and Noguchi and Siemens' F. Blaschke in 1980. Both methods utilized the AC motor drives. DC motor drives was widely used in many industrial applications due to their structure and fast torque dynamic control. But due to its construction of brushed DC motor, the DC motor required regular maintenance such as replacing the carbon brush and it can't operate in high speeds. Slowly AC motor drive become the top choice of many industrial applications due to its low maintenance, high efficiency and tolerate in very high speeds demand.

The first method introduced, Field Oriented Control (FOC), this method is based on two mathematical transformation introduced by Clark and Park. Clark and Park transformation are used in high performance drive or vector control which involved magnet machines. With these the torque and flux will then can be control by using the generated current component, i_{sq}^e and i_{sd}^e in the reference frame. To use FOC method it required the frame transformer, the speed data and current controller to control the torque and flux. Besides, FOC needed a frame transformation to convert the produced current from the excitation frame (i_{sq}^e and i_{sd}^e) to the stationary reference

frame. To convert, it required a complex mathematical calculation and varies sensors. Further detail will be discuss in chapter II.

Later then the Direct Torque Control (DTC) method was introduced. Even though the FOC method provide more advantages most of the companies are then slowly shift from FOC to DTC method. The DTC requires lesser sensitivity on parameter variation to estimate the control parameters. On the other hand, DTC eliminated the use of frame transformation which involved in complex mathematical calculation. Besides using the sensor in DTC, it utilizes the hysteresis controller and a single PI controller to regulate the speed. To establish a fast-instantaneous torque and flux control, a decouple structure is employed and with the present of three-level and two-level hysteresis the torque and flux can be controlled even better.

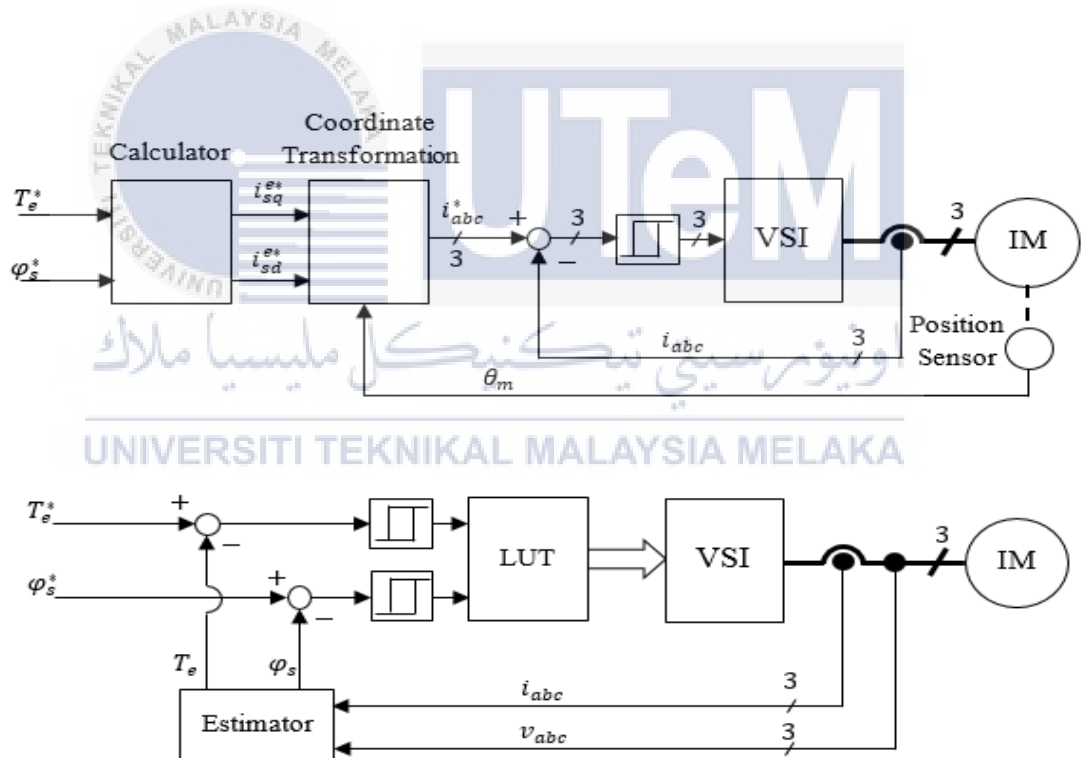


Figure 1: FOC and DTC structure

Although DTC provides various benefits compared to FOC but there is one major drawback of DTC, large torque ripple and variable switching frequencies. There are many modifications been proposed from many areas to minimize the torque ripple and the problem in switching frequencies. Among all the modification proposed, the Space Vector Modulation (SVM) has gained the interest of the public and widely acceptance due to its offer great reduction of torque ripple and a constant switching frequency. Even though this modification, SVM, offered a great improve to DTC but at the same time it increases the complexity and leads to the inaccurate of the performance in control as well as the dynamic torque control.

1.2 Problem statement

With the comparison between DTC and FOC, it clearly shows that the DTC provides more advantages over FOC. Although the DTC offers these advantages and a simple control structure with fast dynamic control but with the use of hysteresis controller come with a next problem, namely large torque ripple and variable inverter switching frequencies. These problems are due to the digital implementation of hysteresis controllers which with a low sampling time. As the sampling time was small it tends to create delay and resulted in torque overshoot the upper band or the lower band of the hysteresis. In the other way it means the torque error are not within the restricted bandwidth of the hysteresis controller. As the torque error are not accurate it will then affect the selections of the voltage vector. The incorrect selection of voltage vector causes the large torque ripples.

Due to the torque slope behaviour, it leads to high switching frequencies as well as the switching losses and hence reduces the efficiency of the inverter. As the power loss emitted in the form on heat, through time the switching devices will degrade and in the end to malfunction.

1.3 Objectives of Research

The objective of this thesis is to reduce the torque ripple and the switching frequencies by implementing dual-inverters for open-end windings induction machine.

1.4 Scopes of Work

The scopes of work for this study are:

- Improve the DTC performances by selecting the most suitable voltage vector.
- To formulate the optimal switching strategy by using a look-up table and modification of torque error status.
- To verify the improvements with simulations and experimentations.

1.5 Research Methodology

A study on the various switching strategies in DTC was carried out in order to understand the how to reduce the torque ripple and maintain a constant switching frequency.

Based on the study, voltage vectors method was the most popular and interested by the public. By selecting the appropriate voltage vector based on the torque error for different speed operation it will certainly help in reducing the torque ripple as well as the switching frequencies. After the justification of torque error, the voltage vector will then be selected by referring to the look-up table.

To obtain constant switching frequencies, the hysteresis controller was then replaced by the constant switching frequency torque controller (CSFTC) to eliminate

the use of PI controller. With CSFTC the major problem in DTC structure can be minimize without changing the entire original DTC structure.

1.6 Thesis Contributions

The research work gave the contribution as follow:

- The torque ripple and switching frequency can be reduce with the appropriate selection of voltage vector.
- The comparison between torque error status and flux error produced by hysteresis controller was made to remain the simple structure of the original DTC design. By then, the use of speed sensor and complex calculation can be eliminated.
- Increase the control bandwidth of DTC by replacing the hysteresis controller with CSFTC and eliminated the use of PI controller.

1.7 Thesis Outline

In this thesis the chapters are:

- Chapter 2 provides an overview of Direct Torque Control structure of induction machine. The parts used in DTC and the mathematical formula were discussed. The basic principle of DTC and the major problems will to be discussed.
- Chapter 3 will explain the detail of methods used to formulate an optimal switching strategy of DTC using dual-inverter for open-end windings induction machine.

CHAPTER 2

LITERATURE REVIEW

2.1 Introduction

In this chapter an overview of Direct Torque Control (DTC) of induction motor will be introduced. DTC method is widely used in many industries as the method used to are much better as compared to the Field Oriented Control (FOC). In this chapter, the control of torque and flux in DTC will be explained and the problem in hysteresis

2.2 Direct Torque Control of Induction Machine

Most of the electric motor drive are implemented with DTC method due to its simpler and effective control method. These methods were introduced by Takahashi and Noguchi in 1986. In DTC hysteresis controller and look-up table are applied. Space Vector Modulation (SVM) was introduced in DTC along with the look-up table to produce fast instantaneous torque and flux control by selecting the suitable voltage vector.

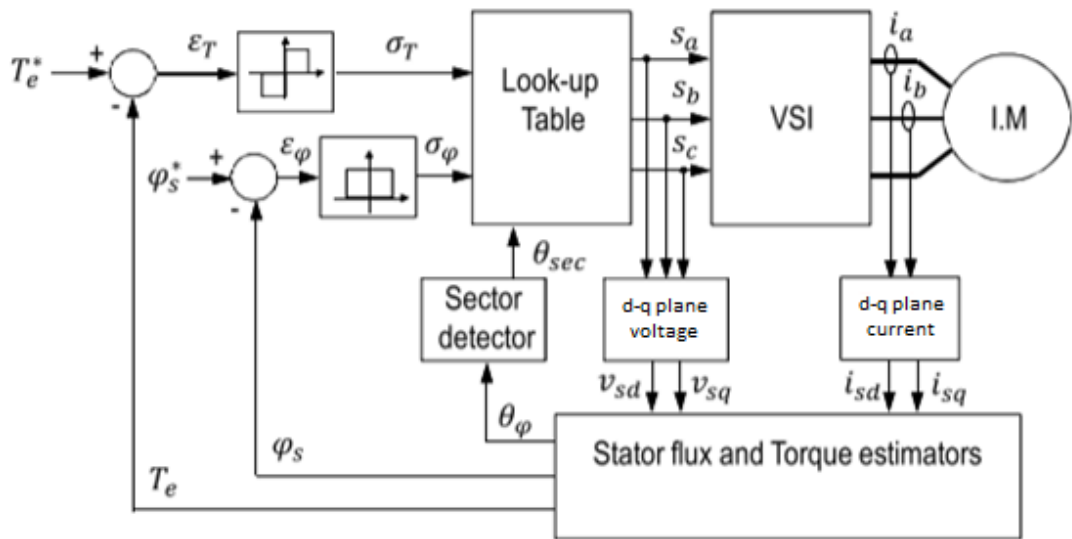


Figure 2: Structure of DTC of Induction Machine

2.2.1 Voltage Source Inverter (VSI)

In this VSI it contains 6 IGBTs. VSI can be used as a toggle switch in the DTC as the switching of the upper IGBTs are complementary to the lower switch. For example, if the switch S1, S3 or S5 switches to high the S2, S4 or S6 will be set to low.

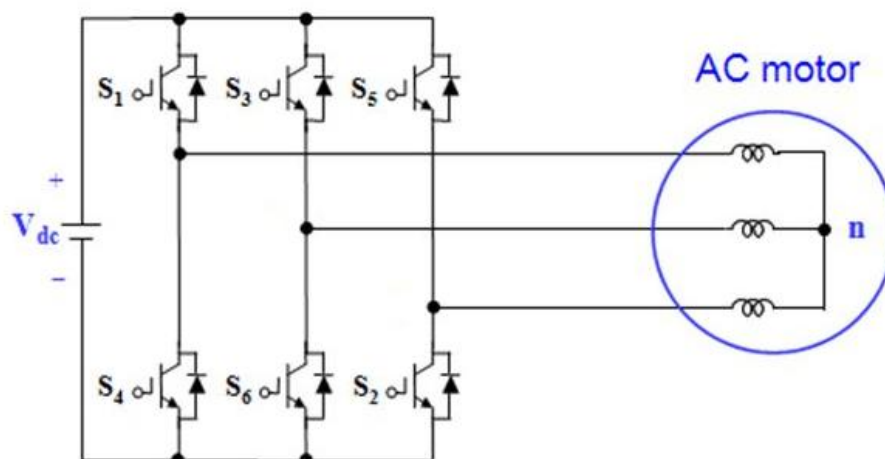


Figure 3: Voltage Source Inverter

The switching state of each IGBT can then form an eight possible switch configuration which then defined as the space vectors. The figure below shows the switching state of S1, S3 and S5 in bracket.

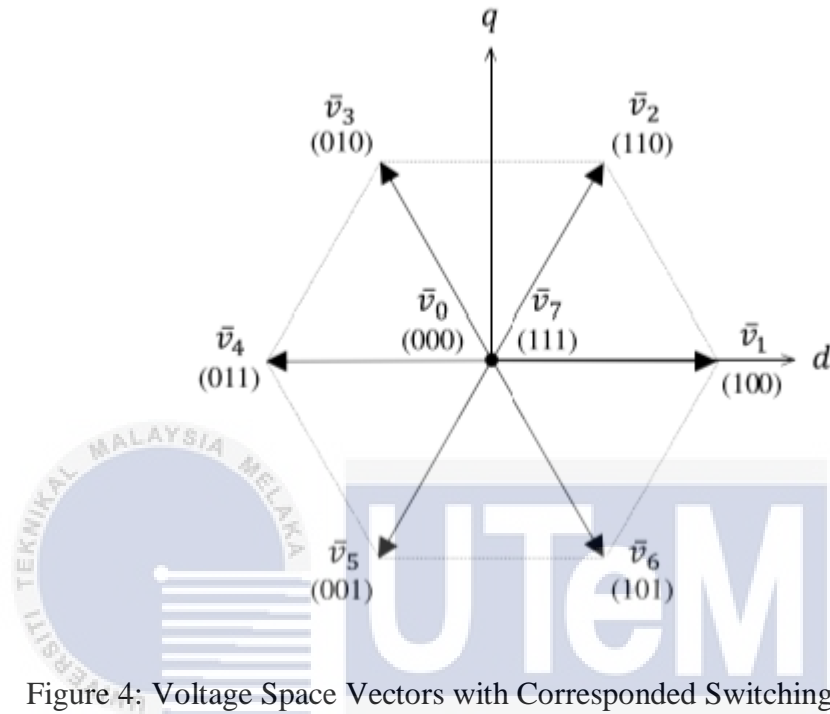


Figure 4: Voltage Space Vectors with Corresponded Switching State

2.2.2 Stator Flux and Torque estimator

To ensure the flux and torque move within the band of the hysteresis an estimator is required to adjust the stator flux and torque. In this estimator few equations are applied to calculate or to determine the stator flux and torque. In the modeling of three phase induction machine an equation was introduced:

$$\tilde{v}_s = R_s \tilde{i}_s + \frac{d\tilde{\varphi}_s}{dt} \quad (2.1)$$

Rearrange this equation to form an integrator for estimating the stator flux:

$$\tilde{\varphi}_s = \int (\tilde{v}_s - R_s \tilde{i}_s) dt \quad (2.2)$$

The estimation of stator flux can be expressed in term of its d-q axis components by separating the real and imaginary part:

$$\varphi_{sd} = \int (\tilde{v}_{sd} - R_s \tilde{i}_{sd}) dt \quad (2.3)$$

$$\varphi_{sq} = \int (\tilde{v}_{sq} - R_s \tilde{i}_{sq}) dt \quad (2.4)$$

To find the stator flux for d-q axis the \tilde{v}_s and \tilde{i}_s parameters must be found, by using

$$i_{sd} = i_a \quad (2.5)$$

$$i_{sq} = \frac{1}{\sqrt{3}}(i_b - i_c) \quad (2.6)$$

$$v_{sd} = \frac{2}{3}(V_{DC})(s_1 - s_2 - s_3) \quad (2.7)$$

$$v_{sq} = \frac{1}{\sqrt{3}}(V_{DC})(s_2 - s_3) \quad (2.8)$$

The i_a , i_b and i_c are the phase current, whereas the s_1 , s_2 and s_3 are the switching status of the IGBTs it will be either 1 or 0 and the V_{DC} is the supplied voltage of the inverter.

2.2.3 Look-up Table

To control the torque and stator flux a suitable voltage vector must be selected. To do so, the switching states of the IGBTs will be represented as the voltage vector as what been discussed in section 2.2.1.

Table 1: Look-Up Table

Stator Flux Error Status, σ_ϕ	Torque Error Status, σ_T	Sector					
		I	II	III	IV	V	VI
1 ($\phi_s \uparrow$)	+1 ($T_e \uparrow$)	\bar{v}_1 (100)	\bar{v}_2 (110)	\bar{v}_3 (010)	\bar{v}_4 (011)	\bar{v}_5 (001)	\bar{v}_6 (101)
	0 ($T_e \downarrow$)	\bar{v}_0 (000)	\bar{v}_7 (111)	\bar{v}_0 (000)	\bar{v}_7 (111)	\bar{v}_0 (000)	\bar{v}_7 (111)
	-1 ($T_e \downarrow\downarrow$)	\bar{v}_5 (001)	\bar{v}_6 (101)	\bar{v}_1 (100)	\bar{v}_2 (110)	\bar{v}_3 (010)	\bar{v}_4 (011)
0 ($\phi_s \downarrow$)	+1 ($T_e \uparrow$)	\bar{v}_2 (110)	\bar{v}_3 (010)	\bar{v}_4 (011)	\bar{v}_5 (001)	\bar{v}_6 (101)	\bar{v}_1 (100)
	0 ($T_e \downarrow$)	\bar{v}_7 (111)	\bar{v}_0 (000)	\bar{v}_7 (111)	\bar{v}_0 (000)	\bar{v}_7 (111)	\bar{v}_0 (000)
	-1 ($T_e \downarrow\downarrow$)	\bar{v}_4 (011)	\bar{v}_5 (001)	\bar{v}_6 (101)	\bar{v}_1 (100)	\bar{v}_2 (110)	\bar{v}_3 (010)

The selection of these voltage vectors will be determined by the stator flux error status and the torque error status. Where the errors are determined by the hysteresis controller.

2.3 Principle of Direct Torque Control

There are 2 parameters being control in DTC, torque and flux. They can be controlled independently or simultaneously using same voltage vectors. It will be divided in to two parts.

2.3.1 Principle of Flux Control

The stator flux can be controlled using the two-level hysteresis controller as shows in figure 2. Based on stator voltage equation (2.1), it can be shown that the variation of flux, $\Delta\bar{\varphi}_s$, is directly affected by the applied voltage vector, where the ohmic drop can be neglected. Hence,

$$\Delta\bar{\varphi}_s \cong \bar{v}_s \cdot \Delta t \quad (2.9)$$

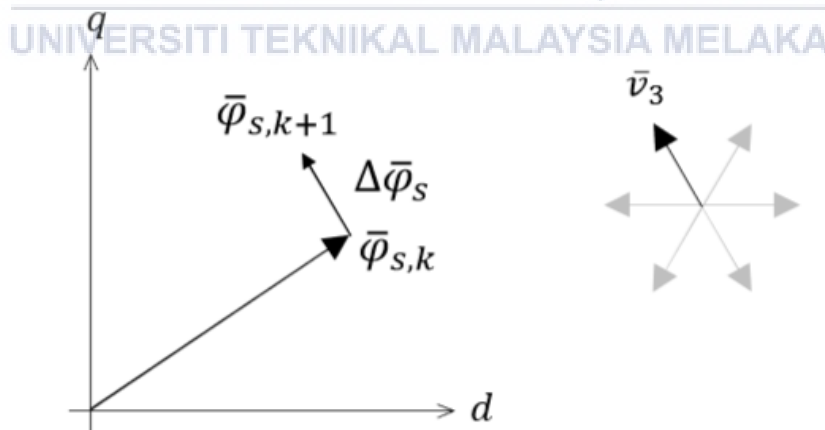


Figure 5: Motion of Stator Flux Vector

The principle of stator flux can be described from figure 5, the trajectory of stator flux is controlled to form a circular locus by controlling the radial component of stator such that its ripple is restricted within the predefined band of the two-level hysteresis controller. The difference between the reference and estimated flux will produce a flux error status, either 0(touches the Upper Band) or 1(touches the Lower Band). When the flux error status is 1, it tends to increase the flux otherwise it will decrease the flux. From figure 4 the locus is located at the origin of the circle; therefore, the locus can be divided in to equally six sectors with six equally to 60° . To increase the stator flux from position $\bar{\varphi}_{s,k}$ to $\bar{\varphi}_{s,k+1}$ required an increment of $\Delta\bar{\varphi}_s$. There are two vectors which allowed the stator flux to move from $\bar{\varphi}_{s,k}$ to $\bar{\varphi}_{s,k+1}$, vector \bar{v}_3 and \bar{v}_4 . In every sector there are two suitable vectors, these vectors are used to control the stator flux. In this case, for \bar{v}_3 is used to increase the stator flux whereas the \bar{v}_4 is used to decrease the stator flux.

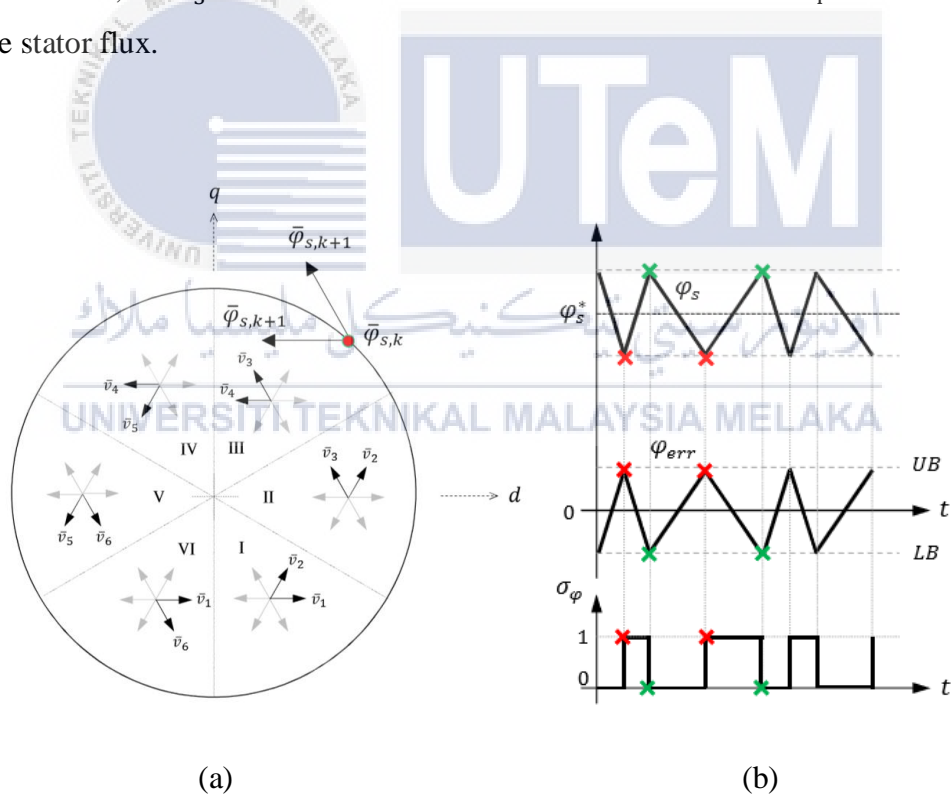


Figure 6: (a) Possible voltage vector for each section, (b) relation between bands and flux error status

2.3.2 Principle of Torque Control

The principle of torque control can be explained if the torque equation,

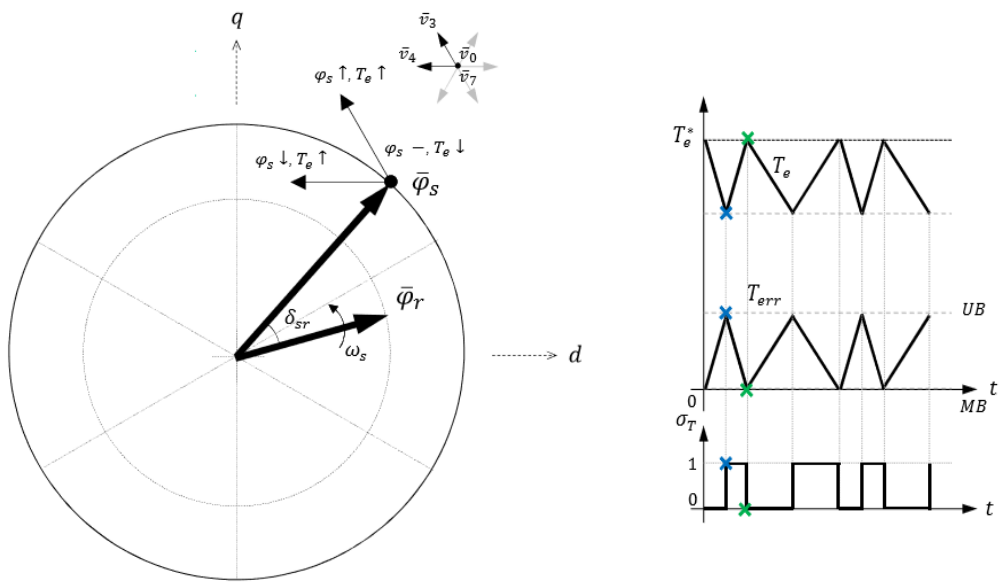
$$T_e = \frac{3}{2}P(\bar{\varphi}_s \times \bar{i}_s) \quad (2.10)$$

Is written into another form, stator flux and rotor flux vector.

$$T_e = \frac{3}{2}P \frac{L_m}{\sigma L_s L_r} |\bar{\varphi}_s| |\bar{\varphi}_r| \sin(\delta_{sr}) \quad (2.11)$$

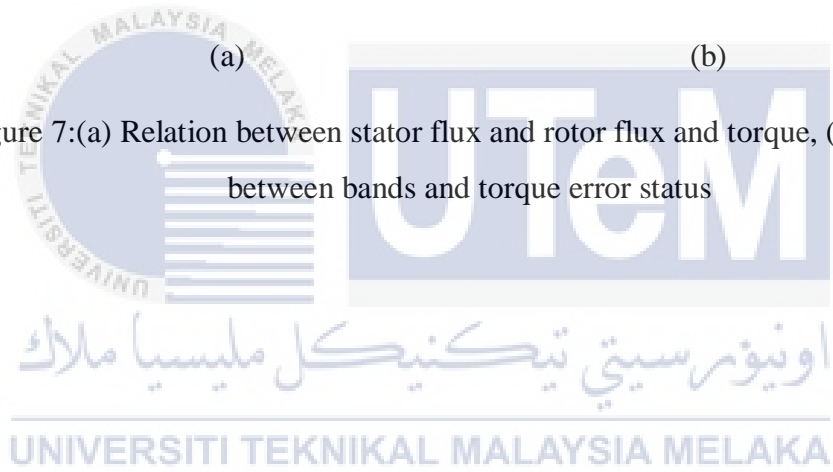
From equation (2.11), it shows that the torque is mainly controlled by the load angle, δ_{sr} , as the other parameters are assumed to be constant. The load angle is the angle between the stator flux and rotor flux vector.

In figure 7, it shows the relation between the stator flux and rotor flux. Assume the rotor flux rotating in a constant angular frequency, ω_e , and the stator flux with different angular frequency due to the applied voltage vector. Which concluded the load angle is mainly affected by the changes of the stator flux vector. Like the principle of flux control, in torque control the torque error status is generated by comparing the reference and estimated torque. The torque error generated is either +3(touches the Upper Band), 0(touches the Middle Band), or -3(touches the Lower Band) due to it utilizing the three-level hysteresis comparator. If the generated torque error status is +3, the DTC tends to increase the torque, 0 tends to decrease the torque whereas when -3 decreases the torque rapidly.



(a) (b)

Figure 7:(a) Relation between stator flux and rotor flux and torque, (b) Relation between bands and torque error status



2.4 Major Problem of Direct Torque Control

In DTC there are 2 drawbacks called large torque ripple and variable switching frequencies.

2.5 Performance Improvements of Direct Torque Control

Throughout the years many methods were proposed to minimize the problems. Some of these methods retain the simple structure of DTC with a minor modification whereas the other proposed methods are more toward on modulation or different control techniques which somehow increase the complexity of the DTC structure. In this sub-chapter will discuss the following proposed methods:

- Space Vector Modulation (SVM)
- Carrier Based Modulation

2.5.1 Space Vector Modulation (SVM)

Among the proposed methods, the SVM method gain the acceptance widely by the researchers for providing constant switching frequency and reduction of torque ripple in DTC. In this method, the space vector modulator replaced the look-up table and hysteresis comparator. This scheme is referred to as DTC-SVM scheme.

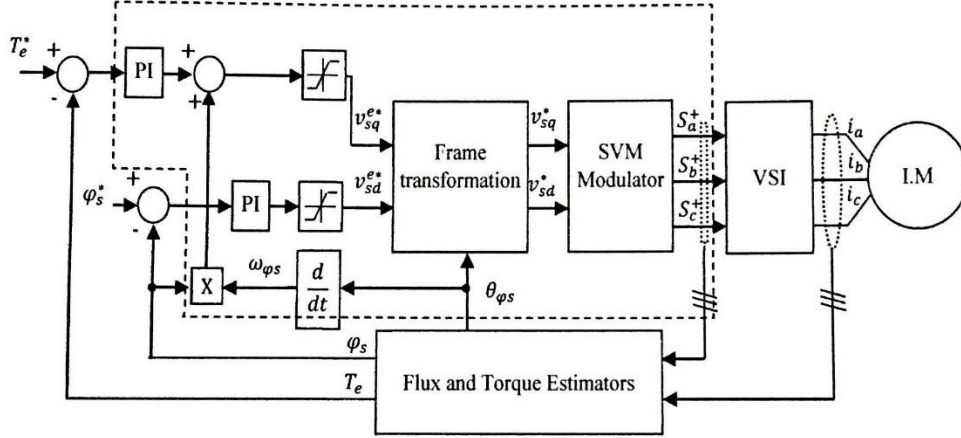


Figure 8: DTC-SVM structure

In this method, the reference voltage has to be estimated to be the input of the modulator. The reference voltage estimated is then synthesized in the modulator to switching the corresponding voltage vector with appropriate switching time, as given in (2.12)

$$\vec{v}_s^* = \vec{v}_{sa} \frac{t_a}{T} + \vec{v}_{sb} \frac{t_b}{T} + \vec{v}_{sz} \frac{t_z}{T} \quad (2.12)$$

Where \vec{v}_{sa} and \vec{v}_{sb} are two adjacent voltage vectors of the reference voltage vector \vec{v}_s^* , and the \vec{v}_{sz} is the zero-voltage vector. Note that, t_a , t_b and t_z are the on-duration for switching the respective vectors \vec{v}_{sa} , \vec{v}_{sb} and \vec{v}_{sz} , where T is the switching period of the modulator. Which satisfied the total time of switching vectors.

$$T = t_a + t_b + t_z \quad (2.13)$$

The reference of space vector based on (2.12) is illustrated in figure 9. In this case, the \vec{v}_s^* is located between the two adjacent vectors $\vec{v}_{sa}=\vec{v}_2$ and $\vec{v}_{sb}=\vec{v}_3$. The

reference of voltage vector can be expressed in term of voltage components as well as given in (2.14).

$$\bar{v}_s^* = \bar{v}_{sd}^* + j\bar{v}_{sq}^* \quad (2.14)$$

Where the d and q axis components of voltage can be obtained from figure 9 using trigonometry theorems as follow:

$$\bar{v}_{sd}^* = |\bar{v}_{sa}| \frac{t_a}{T} + |\bar{v}_{sb}| \frac{t_b}{T} \cdot \cos(60^\circ) \quad (2.15)$$

$$\bar{v}_{sq}^* = |\bar{v}_{sb}| \frac{t_b}{T} \cdot \sin(60^\circ) \quad (2.16)$$

The on-duration for switching the vectors \bar{v}_{sa} , \bar{v}_{sb} and \bar{v}_{sz} can be calculated by determining the magnitude of adjacent voltage vector is constant at $2V_{DC}/3$ and rearranging the equations (2.13),(2.15) and (2.16).

$$t_a = \frac{3}{2} \frac{T}{V_{DC}} \left(v_{s\alpha} - \frac{v_{s\beta}}{\sqrt{3}} \right) \quad (2.17)$$

$$t_b = \sqrt{3} \frac{v_{s\beta}}{V_{DC}} T \quad (2.18)$$

$$t_z = T - t_a - t_b \quad (2.19)$$

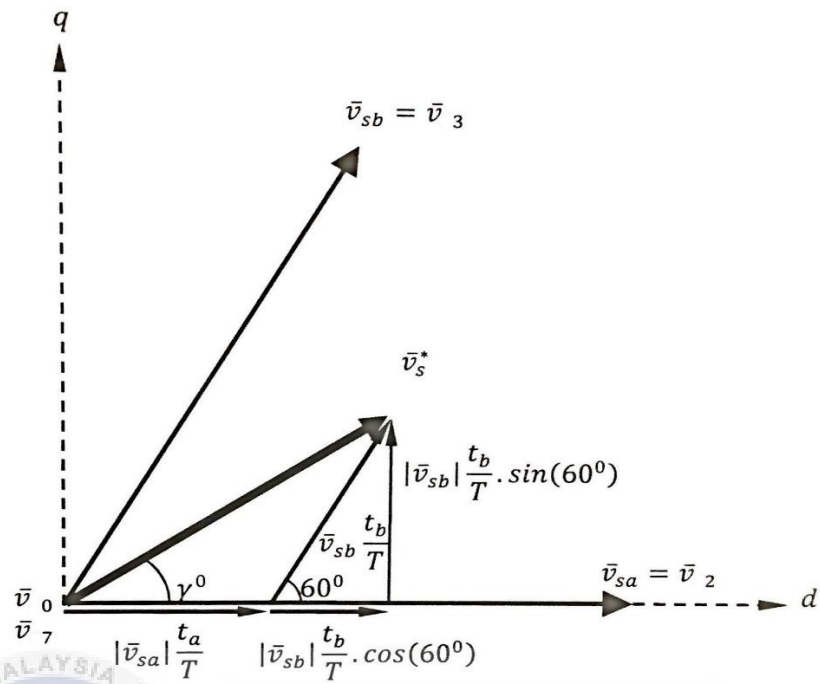


Figure 9: Reference of Space Voltage Vector based on (2.12)

The duty ratio d_1 , d_2 and d_3 were calculated using the on-duration for switching the vectors which were then compared with a carrier waveform to generate switching status, s_1 , s_3 and s_5 to drive the power switches of the inverter.

The torque ripple reduced significantly from figure 10 due to higher number of switching of vectors over one sampling period. It shows that the selections of vectors give an impact to the variation of torque to be regulated closer to its reference.

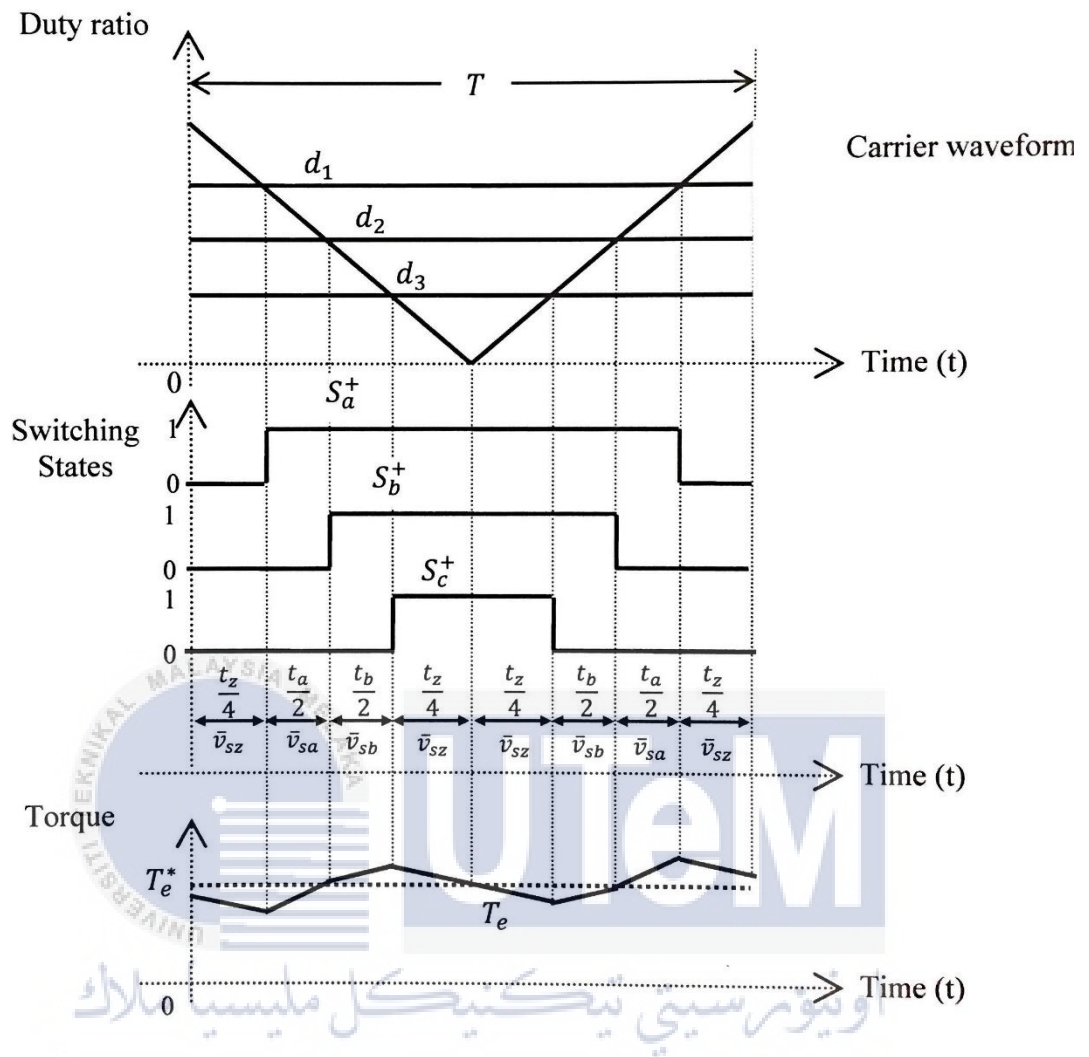


Figure 10: Generation of Switching of Vectors and its Effect on Torque Variations

2.5.2 Carried Based Modulation

Besides, SVM method to reduce the torque ripple it can be obtain by injecting high-frequency triangular waveforms to the errors of torque and flux. This method named as dithering technique, which is simple and effective to minimize the torque ripple even performing DTC at limited sampling frequency. This method offered great reduction of ripple, however it may then produce high switching frequency and leads to higher losses which is not suitable for high power applications.

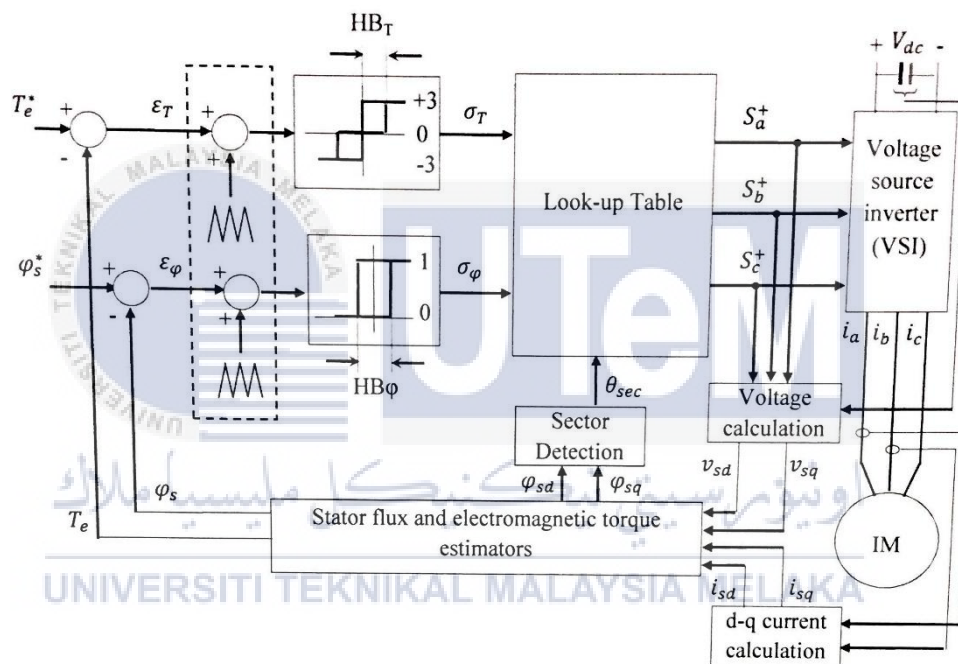


Figure 11: DTC with Dithering Signals Structure

Another simple approach was proposed which the three-level hysteresis comparator was replaced with a constant switching frequency torque controller (CSFTC). It should be noted that the inverter switching frequency is mainly affected by the switching frequency of the torque controller in the DTC scheme.

Later the year, further improvement was made to obtain an exact constant switching frequency by replacing the flux hysteresis comparator with CSFTC. These controllers are based on Field Programmable Gate Arrays (FPGA) which allows the

generations of switching states at high frequency. With these conditions the time for selection of vectors can be minimize and reduce the torque and flux ripples significantly.

Other than operate it in high frequency, the reduction of torque ripple can too be achieved even though running in lower sampling frequency by selecting a suitable gain of PI controller employed in CSFTC.

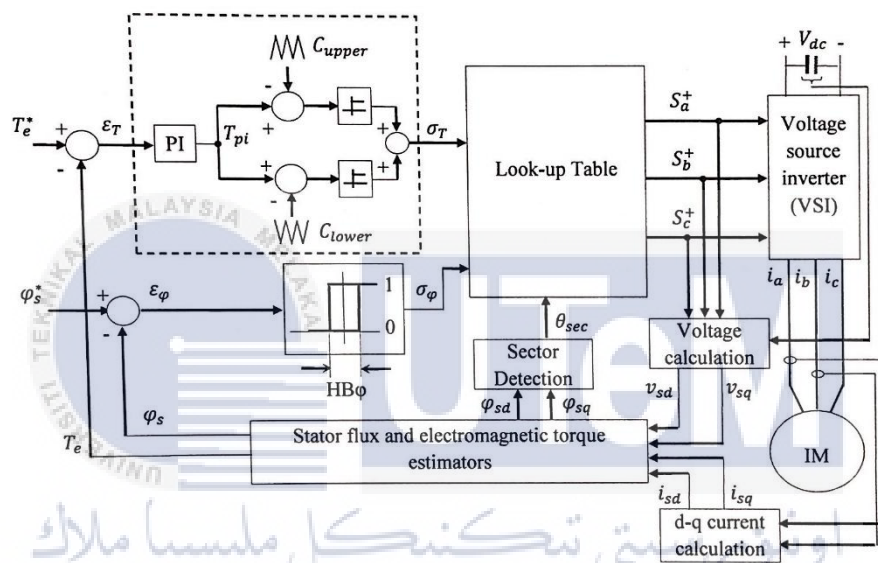
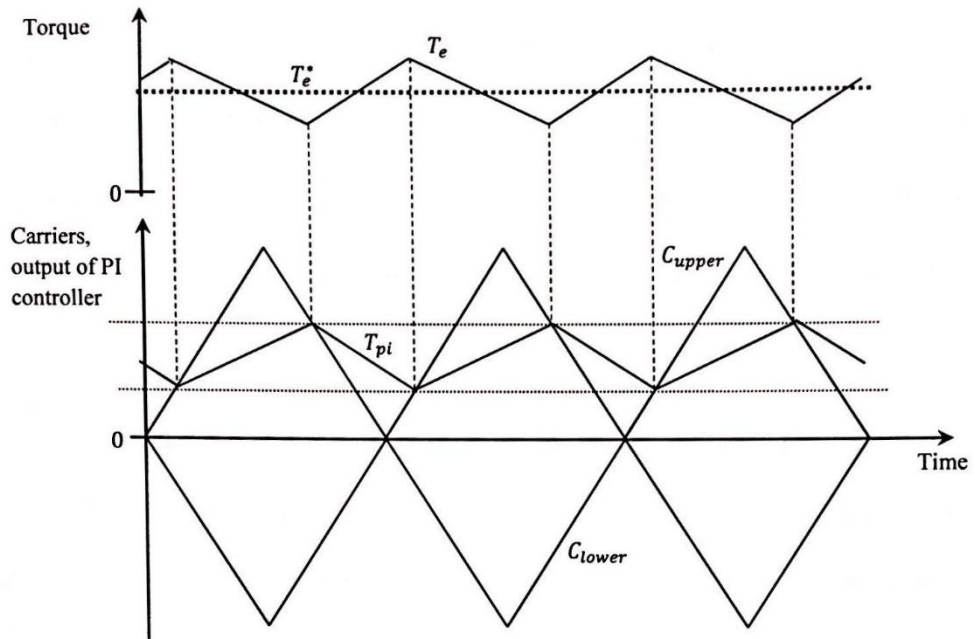
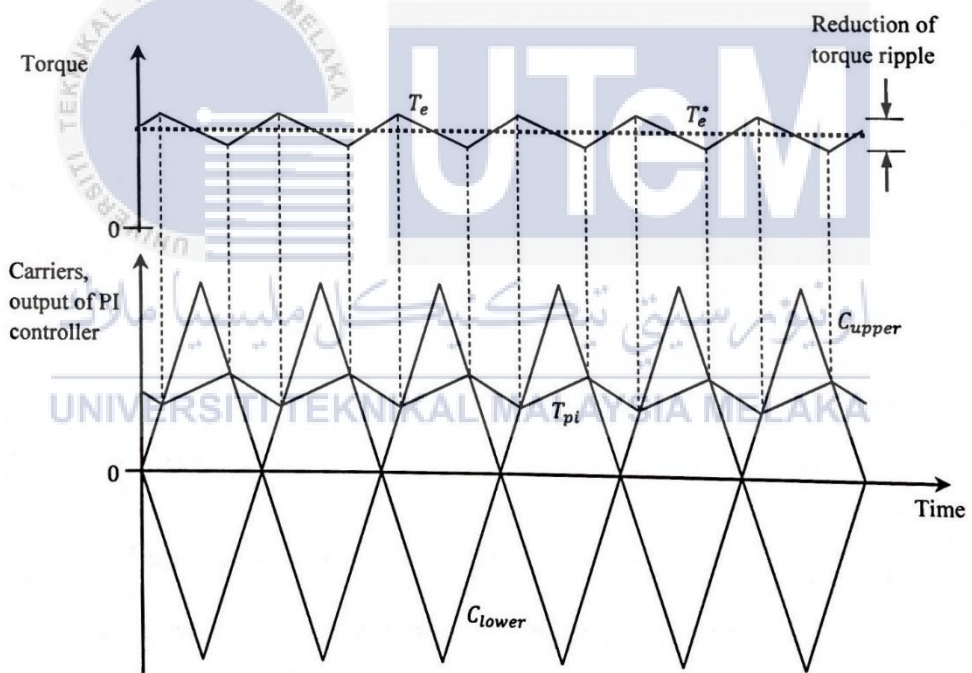


Figure 12: DTC with Constant Switching Frequency Torque Controller



(a)



(b)

Figure 13: Significant Reduction of Torque Ripple with Application of Higher Constant Switching Frequency (a) at Low Carrier Frequency (b) at High Carrier Frequency

This method provided significant improvement with retaining the simple structure of the original DTC scheme, but it requires the knowledge of machine parameters to design a suitable PI controller. Similar to the SVM method, the reduction of torque is obtained by operating the DTC at high switching frequency but the increasing in losses made it not suitable for high power applications.



CHAPTER 3

METHODOLOGY

3.1 Introduction

In this chapter the method used to formulate the proposed optimal switching strategy for open-end windings induction machine using dual-inverter will be discussed. As this proposed method involved induction machine, the mathematical modelling of the induction machine will too be discussed. Besides, the voltage vector available in dual-inverter are mapped into a d-q voltage vector plane by doing this more degrees of freedom will be provided in selecting the most optimal voltage vectors for improving the DTC performance.

3.2 Mathematical Modelling of an Induction Machine

Since the DTC is worked under the stator stationary reference frame it is more beneficial to model the induction machine based on stator stationary reference frame, d-q axis. The induction machine can be expressed using space phasors by the following equations:

Assumption were made to simplify the analysis of the motor model:

- Assuming the rotor using squirrel cage model.
- Rotor and the stator having infinity permeability.
- Flux density radial in the air gap.
- Neglecting the effects cause by slotting, iron loss and end-effects.

$$\bar{v}_s^g = R_s \bar{i}_s^g + \frac{d\bar{\varphi}_s^g}{dt} + j\omega_g \bar{\varphi}_s^g \quad (3.1)$$

$$\bar{v}_r^g = R_r \bar{i}_r^g + \frac{d\bar{\varphi}_r^g}{dt} + j(\omega_g - \omega_r) \bar{\varphi}_r^g \quad (3.2)$$

$$\bar{\varphi}_s^g = L_s \bar{i}_s^g + L_m \bar{i}_r^g \quad (3.3)$$

$$\bar{\varphi}_r^g = L_r \bar{i}_r^g + L_m \bar{i}_s^g \quad (3.4)$$

*superscript 'g' stands for general reference frame.

As these equations are expressed in stationary reference frame, then $\omega_g = 0$ can be written as:

$$\bar{v}_s = R_s \bar{i}_s + \frac{d\bar{\varphi}_s}{dt} \quad (3.5)$$

$$\bar{v}_r = R_r \bar{i}_r + \frac{d\bar{\varphi}_r}{dt} + j\omega_r \bar{\varphi}_r \quad (3.6)$$

$$\bar{\varphi}_s = L_s \bar{i}_s + L_m \bar{i}_r \quad (3.7)$$

$$\bar{\varphi}_r = L_r \bar{i}_r + L_m \bar{i}_s \quad (3.8)$$

By substituting (3.7) into (3.5):

$$\bar{v}_s = R_s \bar{i}_s + \frac{d}{dt} L_s \bar{i}_s + \frac{d}{dt} L_m \bar{i}_r \quad (3.9)$$

By substituting (3.8) into (3.6):

$$\bar{v}_r = R_r \bar{i}_r + \frac{d}{dt} L_r \bar{i}_r + \frac{d}{dt} L_m \bar{i}_s + j\omega_r (L_r \bar{i}_r + L_m \bar{i}_s) \quad (3.10)$$

Putting (3.9) and (3.10) into matrix form with respected to \bar{i}_s and \bar{i}_r :

$$\begin{bmatrix} \dot{i}_s \\ \dot{i}_r \end{bmatrix} = \frac{1}{L_m^2 - L_s L_r} \begin{bmatrix} R_s L_r + j\omega_r L_m^2 & -R_r L_m + j\omega_r L_m L_r \\ -R_s L_m - j\omega_r L_m L_s & R_r L_s - j\omega_r L_r L_s \end{bmatrix} \begin{bmatrix} \bar{i}_s \\ \bar{i}_r \end{bmatrix} + \frac{1}{L_m^2 - L_s L_r} \begin{bmatrix} -L_r & L_m \\ L_m & -L_s \end{bmatrix} \begin{bmatrix} \bar{v}_s \\ \bar{v}_r \end{bmatrix} \quad (3.11)$$

Besides, the motor torque is required since the motor current and rotor speed will be affected by the net torque. The mechanic torque equation:

Mechanical:

$$T_e = J \frac{d\omega_m}{dt} + B\omega_m + T_L \quad (3.12)$$

To develop the electrical torque equation, equation (3.7) will be split into real and imaginary parts as follow:

$$\varphi_{sd} = L_s i_{sd} + L_m i_{rd} \quad (3.13)$$

$$\varphi_{sq} = L_s i_{sq} + L_m i_{rq} \quad (3.14)$$

By substituting the following equations into (3.7),

$$\bar{i}_s = i_{sd} + j i_{sq} \quad (3.15)$$

$$\bar{i}_r = i_{rd} + j i_{rq} \quad (3.16)$$

Then the torque equation for electrical part in term of stator flux and stator current components will be obtained by using a cross product of the stator flux and stator current vectors:

Electrical:

$$T_e = \frac{3}{2} P L_m (i_{sq} i_{rd} - i_{sd} i_{rq}) \quad (3.17)$$

Where B is the vicious friction and ω_m is the mechanical angular speed and J is the moment of inertia.

3.3 Dual Voltage Source Inverters

As for open-end winding induction machine, both sides of the stator windings will be connected to the three-phase voltage with the Voltage Source Inverter (VSI). As shown in Figure 14.

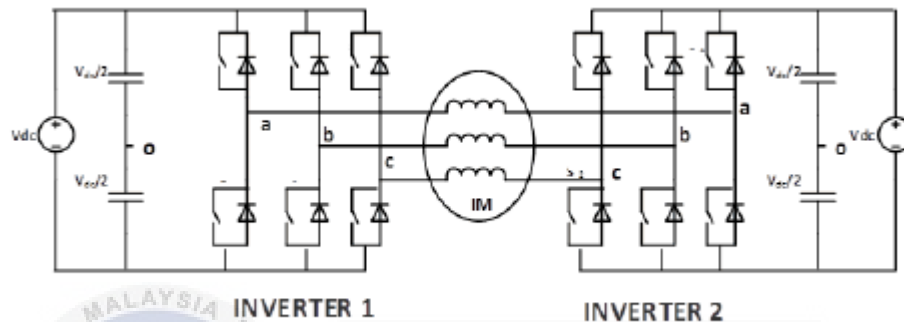


Figure 14: Dual Voltage Source Inverter configuration with Open-End Winding

It has to be made sure that the upper switch does not switch at the same time as the bottom switch. If the upper switch set to 1 the bottom switch has to switch to 0 or off, for avoiding short circuit conditions.

By using dual-inverter, the voltage vector provided are more as compare to the conventional DTC model, a greater number of selections of voltage vector the better the performance of the DTC.

Although there are 64 voltage vectors offered using dual-inverters but only 19 voltage vectors are used. These offered voltage vectors each having their very own characteristic. For example, the flux control vector, torque control vector in the category of short, medium and long vector. As compared to the conventional DTC, the dual-inverters method offered a lower switching loss. In space phasor equations, the space phasor is a means of representing any of the three phase variables, current, voltage and flux by a single vector which rotates in space and is valid for both steady state and transient operations. Once the space phasor forms, then it can be express in the form of d-q axis.

$$\bar{x} = \frac{2}{3}(x_a + \bar{a}x_b + \bar{a}^2x_c) \quad (3.18)$$

To express in d-q axis, the space phasor can be conveniently expressed as follow:

$$\bar{x} = (x_d + jx_q) \quad (3.19)$$

By separating (3.18) into d-q axis,

$$\begin{aligned} x_d &= \text{Re}[\bar{x}] = \text{Re}\left[\frac{2}{3}(x_a + \bar{a}x_b + \bar{a}^2x_c)\right] \\ &= \frac{2}{3}\left(x_a - \frac{1}{2}x_b - \frac{1}{2}x_c\right) \end{aligned} \quad (3.20)$$

$$x_d = \text{Im}[\bar{x}] = \text{Im}\left[\frac{2}{3}(x_a + \bar{a}x_b + \bar{a}^2x_c)\right] = \frac{1}{\sqrt{3}}(x_b - x_c) \quad (3.21)$$

Applying (3.20) and (3.21), the stator voltage vector components can be written as:

$$v_{sd} = \frac{2}{3}\left(v_{an} - \frac{1}{2}v_{bn} - \frac{1}{2}v_{cn}\right) \quad (3.22)$$

$$v_{sq} = \frac{1}{\sqrt{3}}(v_{bn} - v_{cn}) \quad (3.23)$$

In term of switching status, the stator voltage vector components in (3.22) and (3.23) can be written as:

$$v_{sd} = \frac{2}{3}V_{DC}\left(S_a - \frac{1}{2}S_b - \frac{1}{2}S_c\right) \quad (3.24)$$

$$v_{sq} = \frac{1}{\sqrt{3}}V_{DC}(S_b - S_c) \quad (3.25)$$

Applying the (3.24) and (3.25) in the simulation for both inverters,

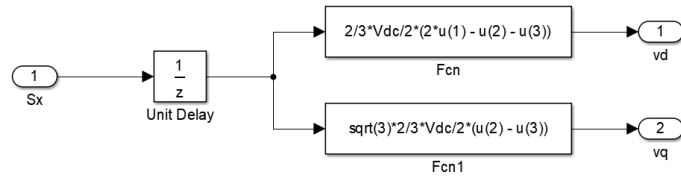


Figure 15: Dual Voltage Source Inverter Schematic (Inverter 1)

3.4 Proposed Optimal Switching Strategy

It is important to understand the effects of torque variations for every application voltage vector at different speed operation. The effect of voltage vector on the torque variations are investigated to identify the most suitable voltage vector to improve the DTC performance in term of torque ripple reduction and switching frequency.

3.4.1 Principle of Torque Control based on Load Angle, δ_{sr}

The principle of torque can be explained if the torque equation is expressed into another form.

$$T_e = \frac{3}{2}P(\bar{\varphi}_s x \bar{i}_s) \quad (3.26)$$

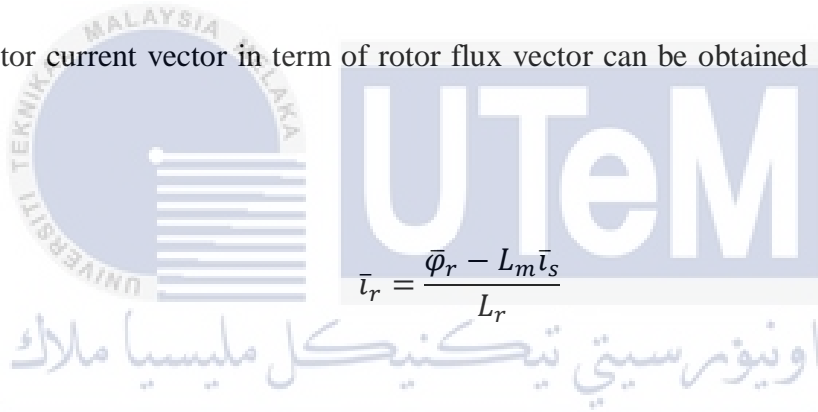
Rearrange the relation in (3.7) into the terms of rotor current vector.

$$\bar{i}_s = \frac{\bar{\varphi}_s - L_m \bar{i}_r}{L_s} \quad (3.27)$$

By considering $\bar{\varphi}_s \times \bar{i}_s = 0$ and substituting (3.27) into (3.26),

$$T_e = \frac{3}{2} P \left(\frac{\bar{\varphi}_s L_m \bar{i}_r}{L_s} \right) \quad (3.28)$$

The rotor current vector in term of rotor flux vector can be obtained by rearranging (3.8),



$$\bar{i}_r = \frac{\bar{\varphi}_r - L_m \bar{i}_s}{L_r} \quad (3.29)$$

Substituting (3.29) into (3.28),

$$T_e = \frac{3}{2} P \left(\frac{\bar{\varphi}_s L_m}{L_s} \right) \left(\frac{\bar{\varphi}_r - L_m \bar{i}_s}{L_r} \right)$$

$$T_e = \frac{3}{2} P L_m \left(\frac{\bar{\varphi}_s \times \bar{\varphi}_r}{L_s L_r} \right) + \frac{3}{2} P L_m^2 \left(\frac{\bar{\varphi}_r \times \bar{i}_s}{L_s L_r} \right) \quad (3.30)$$

From (3.26), it can be rearranged to obtain the cross product of stator flux and stator current vectors,

$$(\bar{\varphi}_s \times \bar{i}_s) = \frac{T_e 2}{3P} \quad (3.31)$$

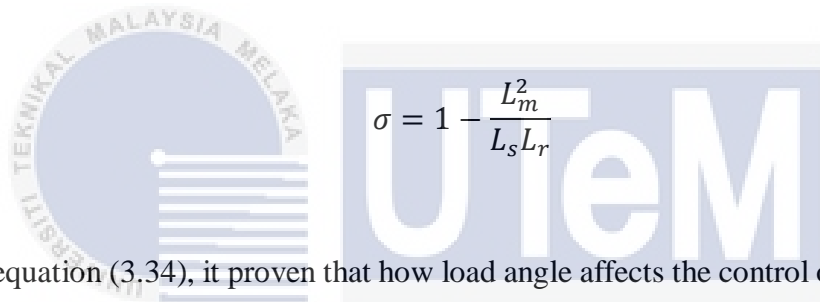
Applying (3.31) into (3.30),

$$T_e = -\frac{3}{2}P \left(\frac{L_m}{\sigma L_s L_r} \right) \bar{\varphi}_s \times \bar{\varphi}_r \quad (3.32)$$

or

$$T_e = -\frac{3}{2}P \left(\frac{L_m}{\sigma L_s L_r} \right) |\bar{\varphi}_s| \cdot |\bar{\varphi}_r| \sin(\delta_{sr}) \quad (3.33)$$

Where, δ_{sr} is the angle difference between the stator flux vector and the rotor flux vector and σ is total leakage factor which is given by:



$$\sigma = 1 - \frac{L_m^2}{L_s L_r} \quad (3.34)$$

From equation (3.34), it proven that how load angle affects the control of torque. With (3.34) the relation between torque and load angle will be, the greater the load angle, the greater the torque. By selecting a forward leading voltage vector, the load angle will increase. On the other hand, the torque can be reduced quickly by reducing the load angle by selecting a backward voltage vector and to reduce the torque with a slower rate the zero-voltage vector will be the best fit. The diagram below will give a better idea on how voltage vector affecting the load angle and lead to increase or decrease torque.

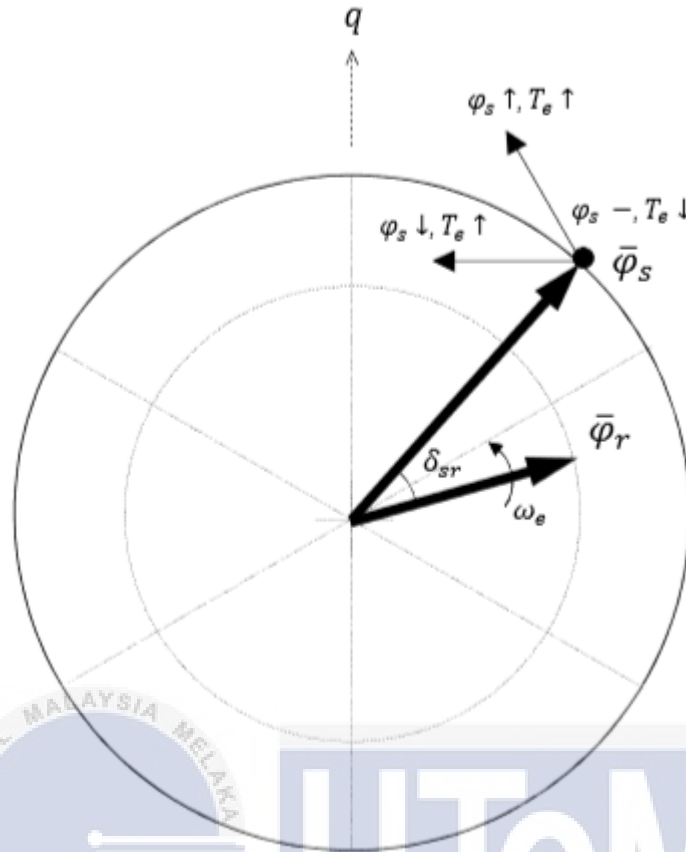


Figure 16: Relation between selection of vector and torque and flux status

3.5 Definition of Flux Sectors for Selecting Optimal Voltage Vectors

There are two type of flux sector as this method implementing dual-inverters. In Figure 17, it shows the long/short and medium voltage vector flux sector. In the 12 long and short voltage vectors, they are all aligned with same angle and rotation but different in amplitude. On the other hand, in the medium voltage vector flux sector, it contains 6 medium voltage vectors which having 30 difference in angle as compare to the respective long and short voltage vectors. These vectors are used to increase or decrease the torque or stator flux.

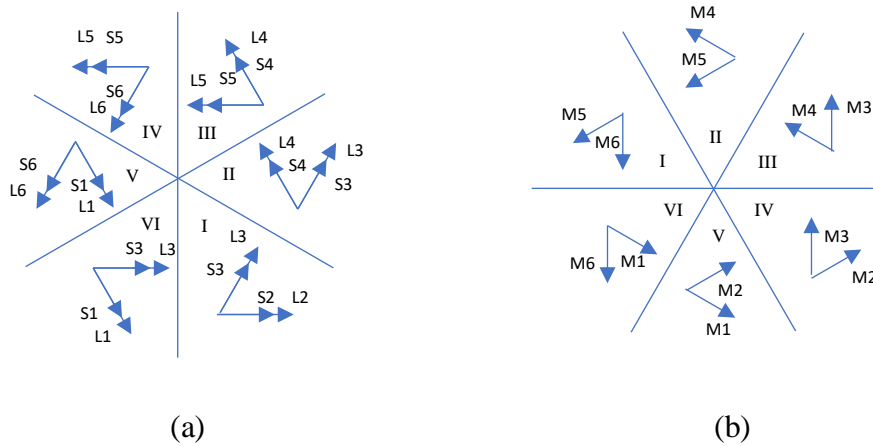


Figure 17: Flux sector and suitable Voltage Vector for (a) Long/Short (b) Medium

In figure 17, it shows the suitable vectors for each sector for long/short and medium. The vectors will be discussing later in Look-up Table.

3.6 Look-up Table for Selecting Optimal Voltage Vector

According to Takashi and Noguchi, the voltage vector used to increase the torque should have more tangential component to the flux vector and the most radial component to the stator flux vector must avoided. In the proposed method, it has differences, it offers more voltage vector with different amplitude, the short, medium and long. There is more option in this proposed method for reducing the rate of change of torque as well as switching frequency.

Table 2: Look-up Table for Selection Optimal Voltage Vectors in Dual-Inverters

Stator Flux Error status, σ_ϕ	Modified torque error status, σ_T^\pm	Sector I	Sector II	Sector III	Sector IV	Sector V	Sector VI
1	3	L2 [100101]	L3 [101001]	L4 [011001]	L5 [011010]	L6 [010110]	L1 [100110]
	2	M5 [010010]	M4 [011000]	M3 [001001]	M2 [100001]	M1 [100100]	M6 [000110]
	1	S2 [000101]	S3 [101000]	S4 [010001]	S5 [001010]	S6 [010100]	S1 [100010]
	0	Z0 [010101]	Z0 [101010]	Z0 [010101]	Z0 [101010]	Z0 [010101]	Z0 [101010]
	-1	S6 [010100]	S1 [100010]	S2 [000101]	S3 [101000]	S4 [010001]	S5 [001010]
	-2	M3 [001001]	M2 [100001]	M1 [100100]	M6 [000110]	M5 [010010]	M4 [011000]
	-3	L6 [010110]	L1 [100110]	L2 [100101]	L3 [101001]	L4 [011001]	L5 [011010]
0	3	L3 [101001]	L4 [011001]	L5 [011010]	L6 [010110]	L1 [100110]	L2 [100101]
	2	M6 [000110]	M5 [010010]	M4 [011000]	M3 [001001]	M2 [100001]	M1 [100100]
	1	S3 [101000]	S4 [010001]	S5 [001010]	S6 [010100]	S1 [100010]	S2 [000101]
	0	Z0 [101010]	Z0 [010101]	Z0 [101010]	Z0 [010101]	Z0 [101010]	Z0 [010101]
	-1	S5 [001010]	S6 [010100]	S1 [100010]	S2 [000101]	S3 [101000]	S4 [010001]
	-2	M2 [100001]	M1 [100100]	M6 [000110]	M5 [010010]	M4 [011000]	M3 [001001]
	-3	L5 [011010]	L6 [010110]	L1 [100110]	L2 [100101]	L3 [101001]	L4 [011001]

3.7 Proposed Control Structure

Figure 18 shows the control structure of the proposed method of DTC using dual-inverters for open end winding induction motor. The proposed method keeping most of the conventional DTC structure. The difference between the proposed method and the conventional DTC is in proposed method it is utilizing dual-inverters.



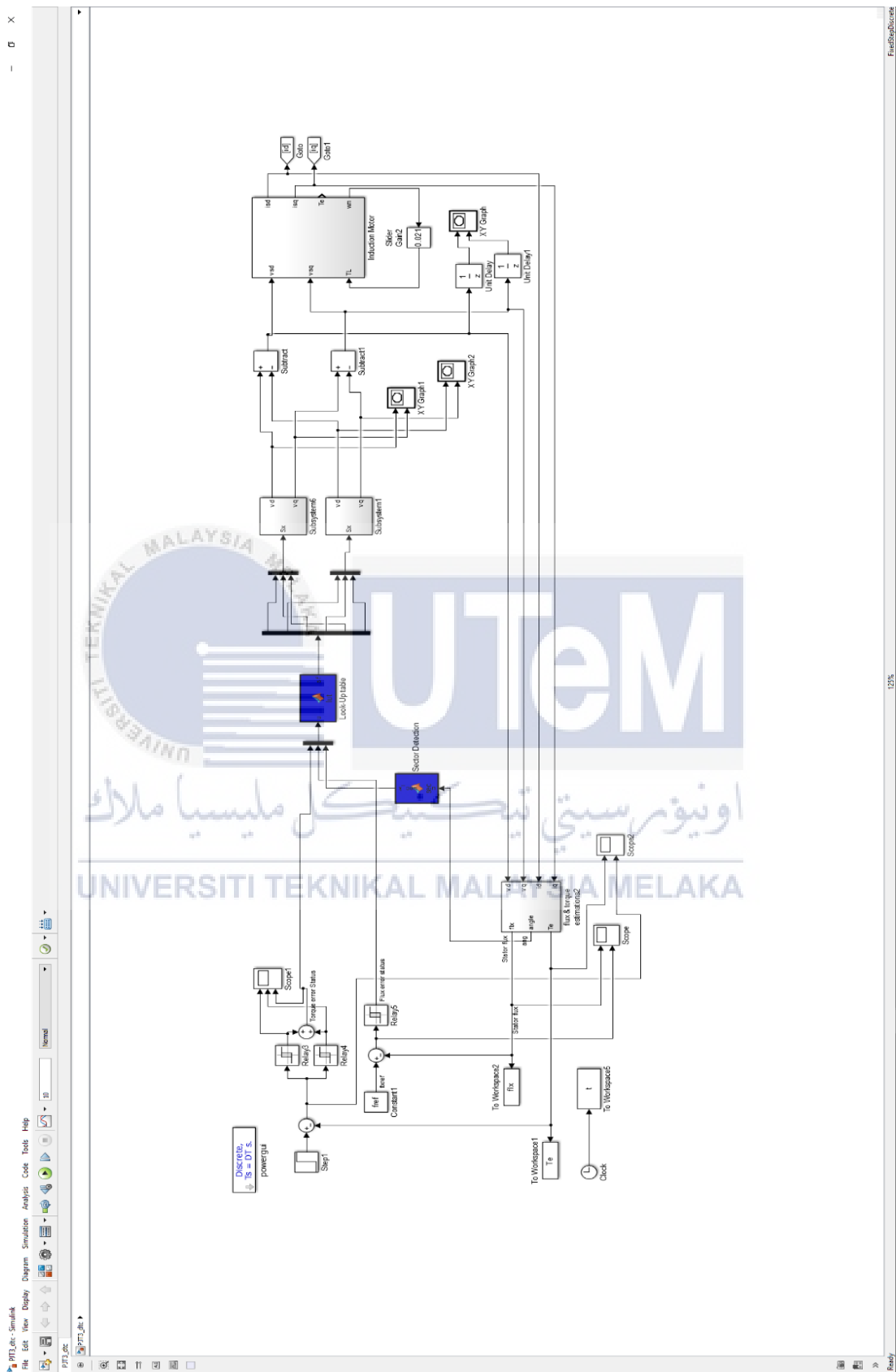


Figure 18: Proposed Control Structure of DTC

CHAPTER 4

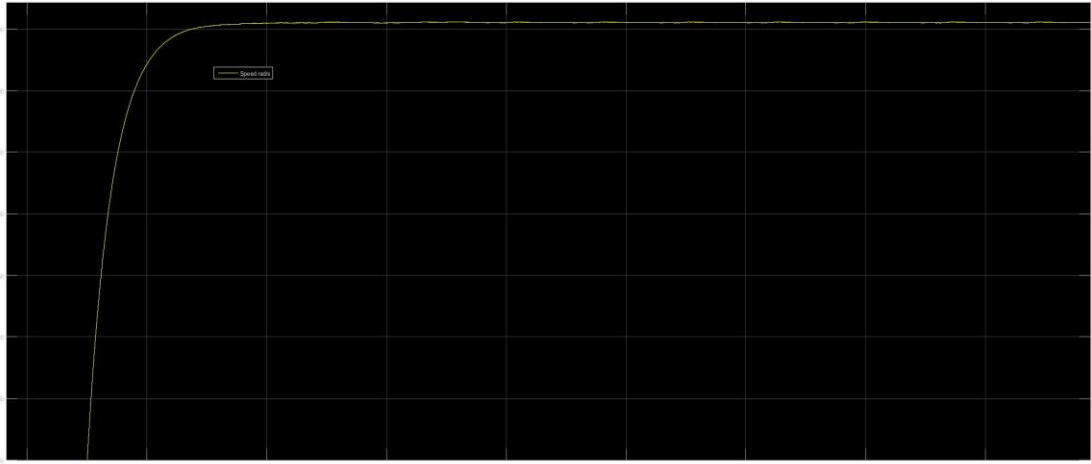
Result and Discussion

4.1 Introduction

In the chapter, it will be focus on the result obtained via the simulations and test run to highlight how the proposed method performance are better compared to the conventional DTC.

4.2 Torque Ripple Reduction and Switching Frequency Reduction

To reduce the torque ripple and the switching frequency, an appropriate voltage vector will be the main factor as shown in Chapter 3. To justify the proposed method working in reducing the torque ripple and switching frequencies, tests were carried out at constant reference torque for all low speed, medium speed and high-speed operation. In Figure 19, it shows the torque, currents and phase voltage waveform obtaining from the simulation in the low speed operation. The operation speed is around 92rad/s (879rpm) as shown in Figure 19.



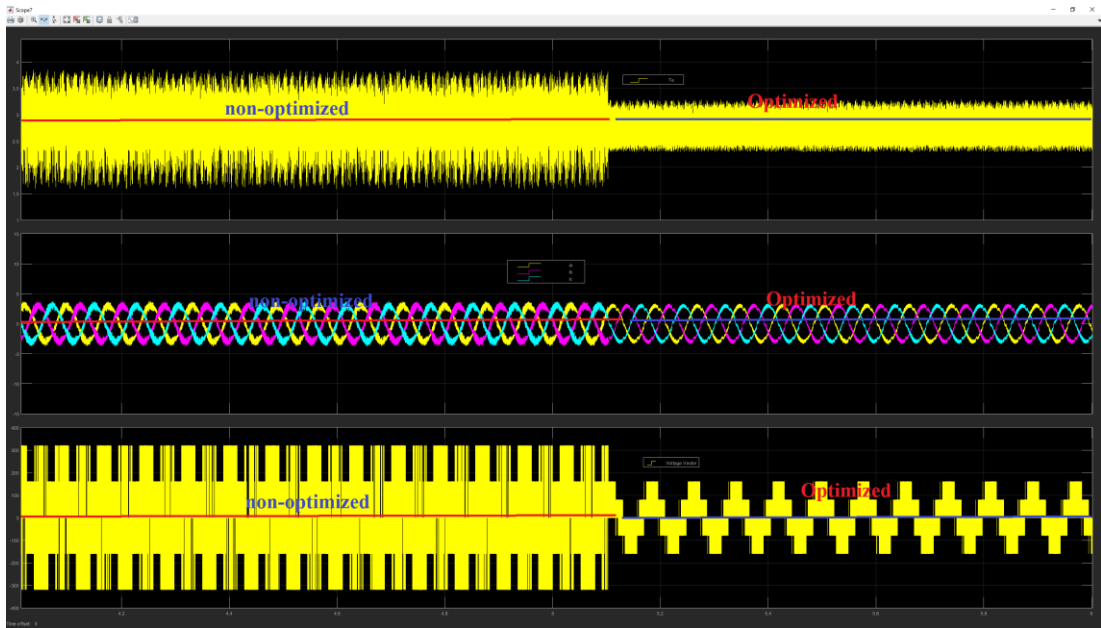
(a)



(b)

Figure 19: Speed of the motor 92rad/s (a) general view (b) Zoomed version

The result obtained from the simulation in Figure 20 initially was running under the non-optimized switching mode, from there it can be observed that the torque ripple is very big but when the optimized method applied it can be seen that the torque ripple was reduced significantly as the rate of increase of torque is slower. The effect of torque increases due to appropriate vector selection. In Figure 20 (b), it can be observed that the switching indicated by regulation of torque is less often with the optimal switching. Which implies, the selection of short voltage vector can greatly reduce the slope of torque increase mainly contributes the reduction of switching frequency. Besides, in the phase currents, it too can be observed that the ripple of the 3 currents are very high as well, with the aids of proper voltage selection, i.e. short voltage vector, the ripple was reduced. On the other hands, phase voltage, before the optimized method applied, the phase voltage having different amplitude of fundamental components. When the optimized method applied, the phase voltage exhibits in a lower amplitude as the selection of voltage vector was short to increase the torque and zero-vector to decrease the torque whereas the conventional DTC select long voltage vector to increase the torque and zero-vector to decrease the torque. Figure 21 shows the operation speed for the medium speed test; the speed is around 123rad/s (1175rpm). In Figure 22, it shows the waveforms of torque, currents and phase voltage from the simulation. Same condition was applied as in the low speed operation. The simulation was initially run under non-optimized condition where it is utilizing the conventional DTC setting. As in Figure 22 the non-optimized and optimized waveforms of respective elements. From Figure 22 (a), the torque ripple reduced as the proposed method applied. Similar improvements obtained for the phase currents and phase voltage. For the high-speed operation at 140rad/s (1337rpm), similar result is obtained as well in reducing the torque ripple and switching frequency in Figure 24.



(a)



(b)

Figure 20: Waveforms of Torque (T_e), Phase Currents (i_a , i_b , i_c) and Phase Voltage with non-optimized and optimized switching at Low-Speed Operation. (a) General view (b) the zoom-in version

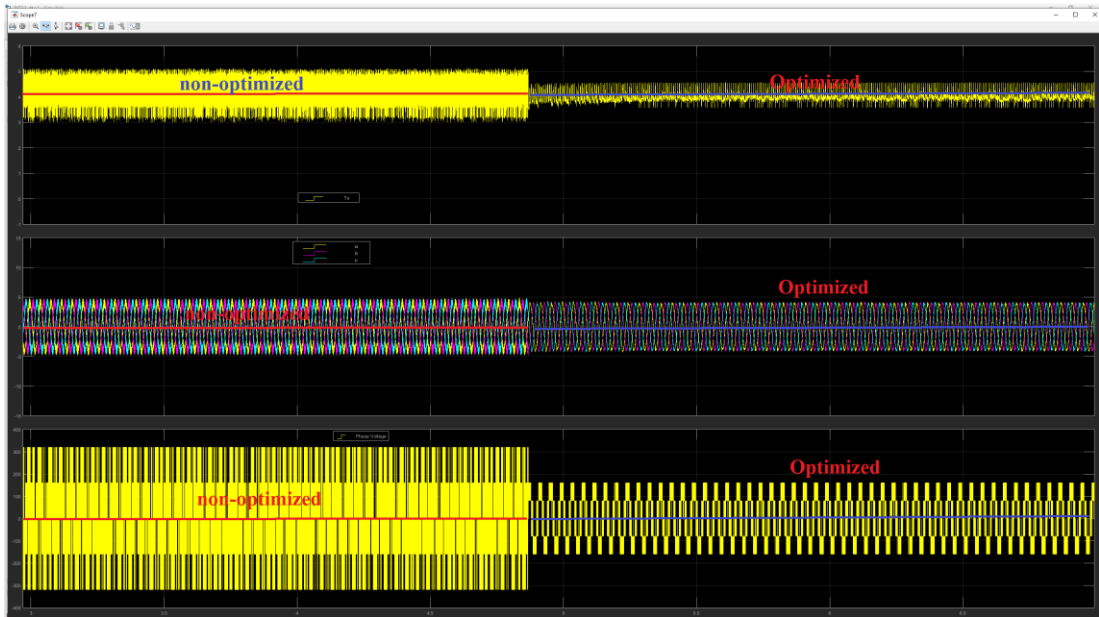


(a)

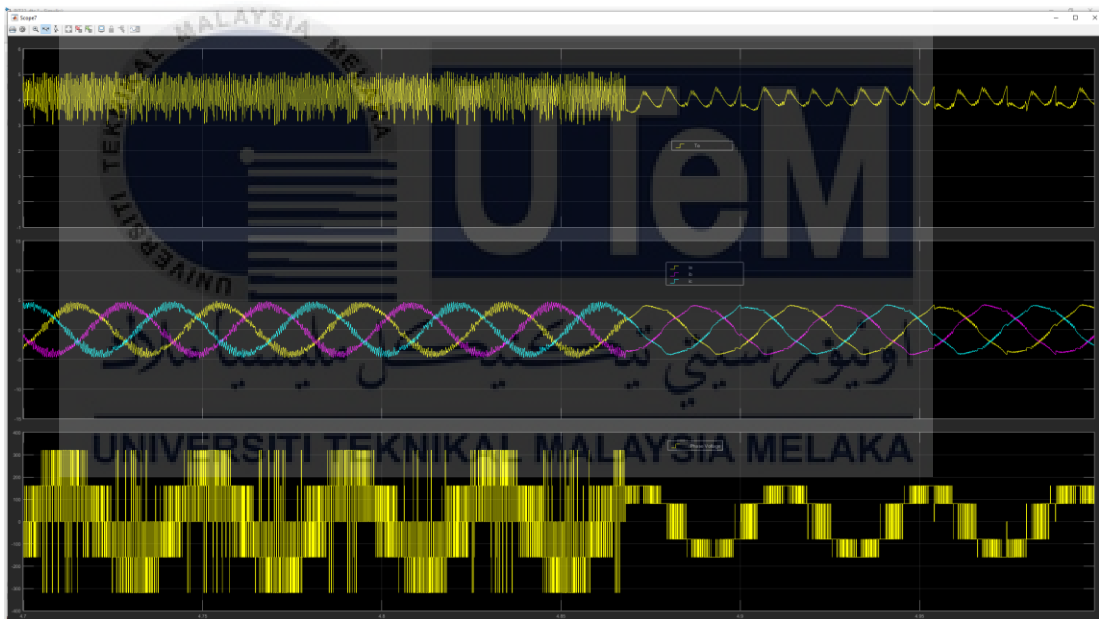


(b)

Figure 21: Speed of the motor 123 rad/s (a) general view (b) Zoomed version



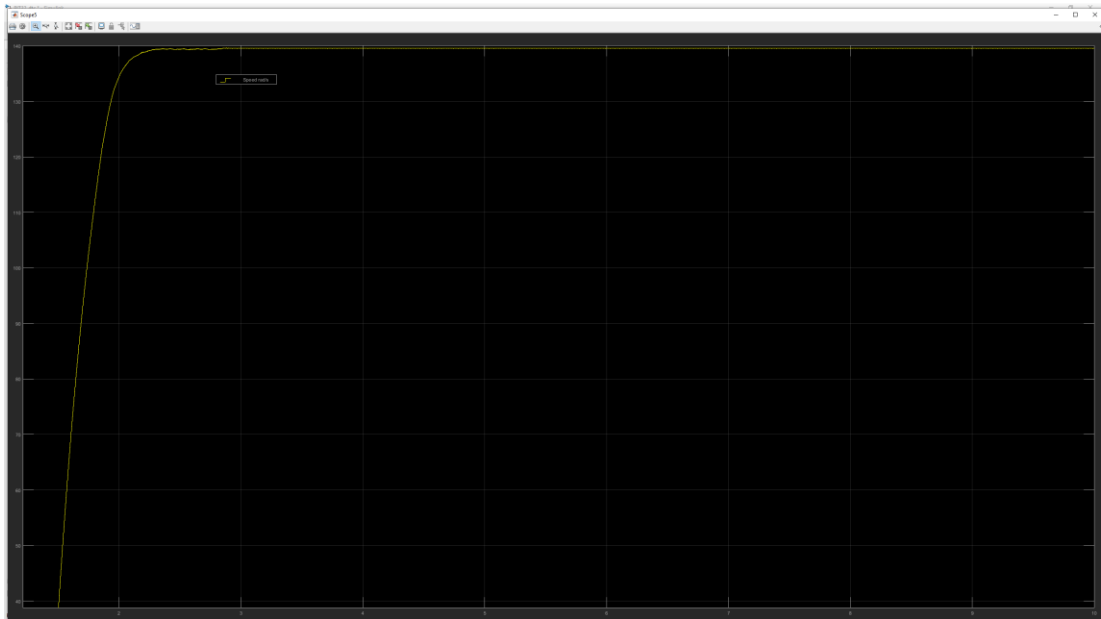
(a)



(b)

Figure 22: Waveforms of Torque (T_e), Phase Currents (i_a , i_b , i_c) and Phase Voltage with non-optimized and optimized switching at Medium-Speed Operation. (a)

General view (b) the zoom-in version

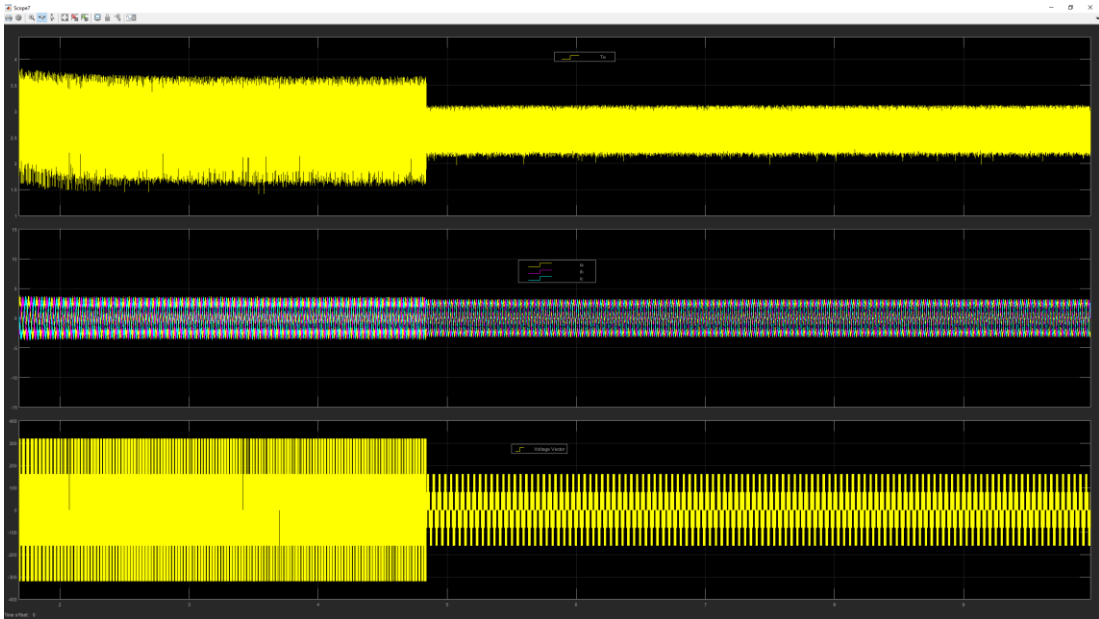


(a)

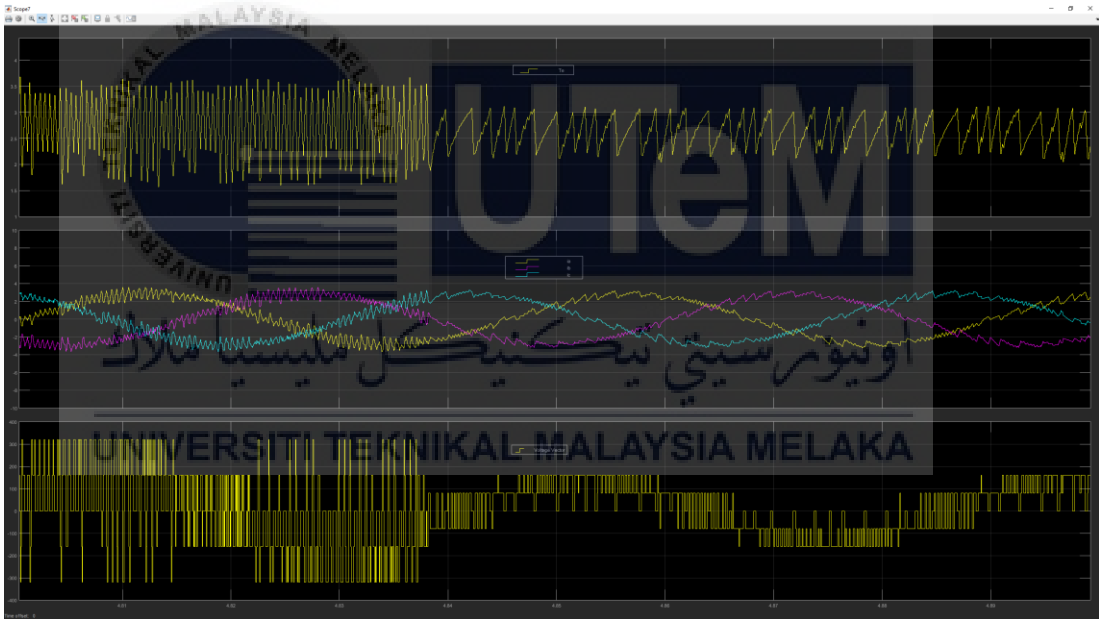


(b)

Figure 23: Speed of the motor 140rad/s (a) general view (b) Zoomed version



(a)

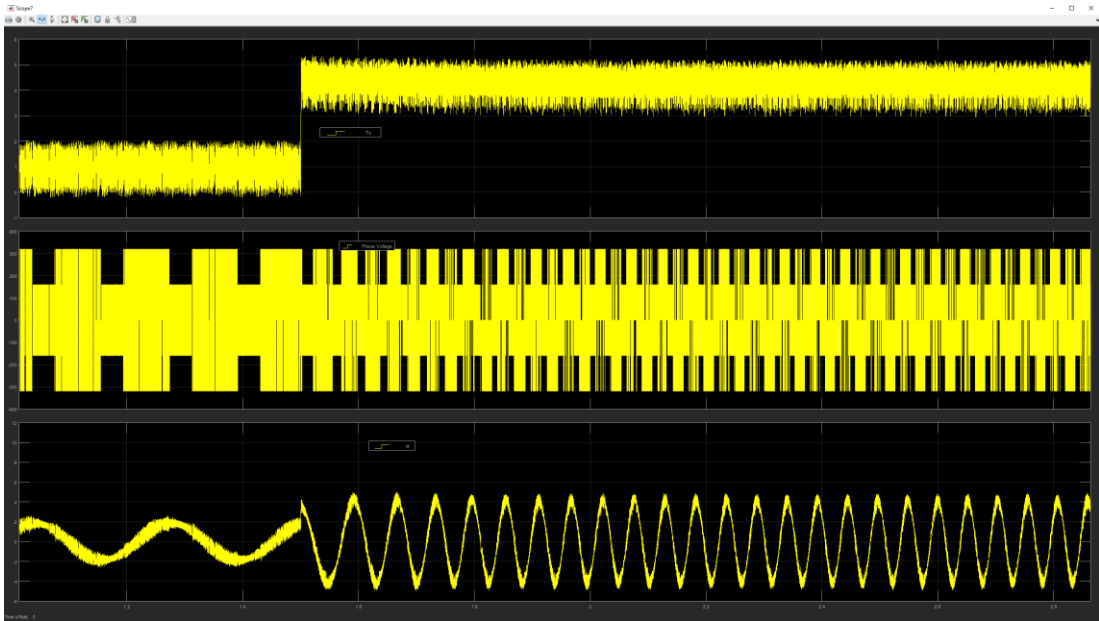


(a)

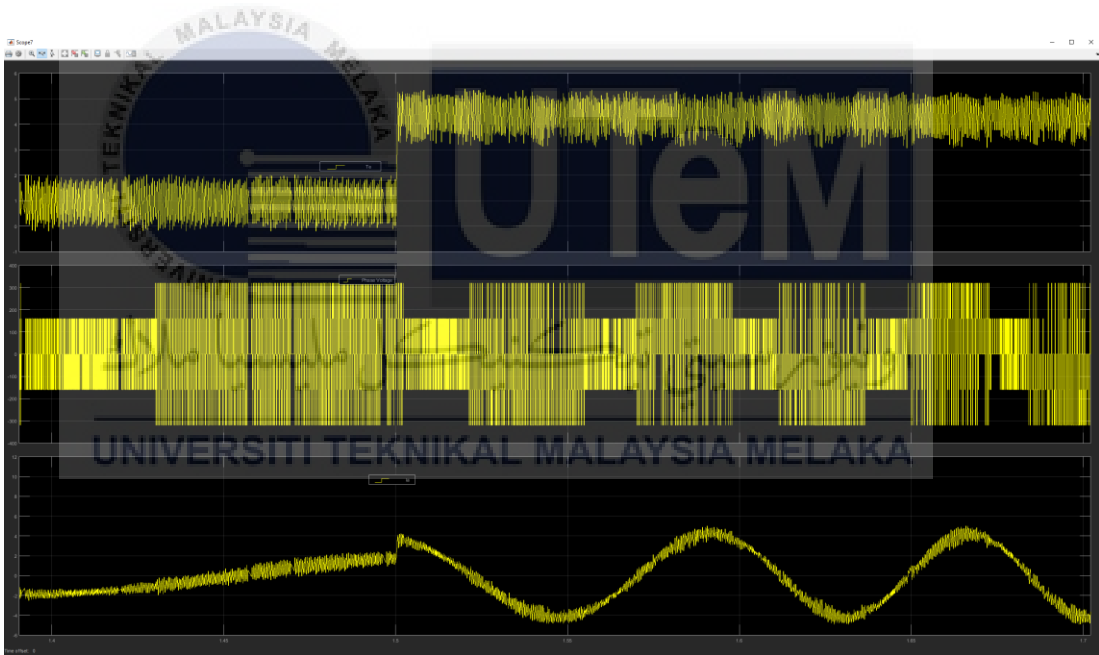
Figure 24: Waveforms of Torque (T_e), Phase Currents (i_a , i_b , i_c) and Phase Voltage with non-optimized and optimized switching at High-Speed Operation. (a) General view (b) the zoom-in version

4.3 Reduction of Torque Ripple and Switching Frequency for a Torque Dynamic Control

The use of optimal switching strategy can be applying under torque dynamic condition as well. Under the dynamic condition, the effect of optimal switching strategy can be even display clearer by determining the appropriate voltage vector for reducing the torque ripple and the switching frequency under different speed. In Figure 25 to Figure 27 shows the waveform of torque, phase voltage and phase current for a step change of reference torque in DTC with non-optimized switching strategy at low, medium and high speed. As a step change in the reference torque it will accelerate the motor speed which can be seen through the increase of the phase current frequency. Notice that the amplitude or the peak of the phase voltage waveform remaining the same throughout the entire operation for various speed. Considering the non-optimized switching utilizing the long voltage vector to increase the torque and zero vector to decrease the torque for all type of speed. Since the selected voltage vector is not appropriate, therefore the torque ripple and switching frequency will appear in a large manner throughout the entire operation or process. The effect of inappropriate voltage vector selection can be shown by magnifying the waveform of Figure 25 to Figure 27. These magnified images are display as (b) from Figure 25 to Figure 27. From Figure 28 to Figure 30 shows the waveforms torque, phase voltage and phase current for the step change of reference torque of the simulation using the DTC with optimized switching strategy. With the suitable voltage vector selected for respective operating condition, where the decrease or increase of torque are determined by the respective vector resulted in torque ripple reduction and switching frequency reduction as compared to the waveforms obtained with non-optimized DTC.

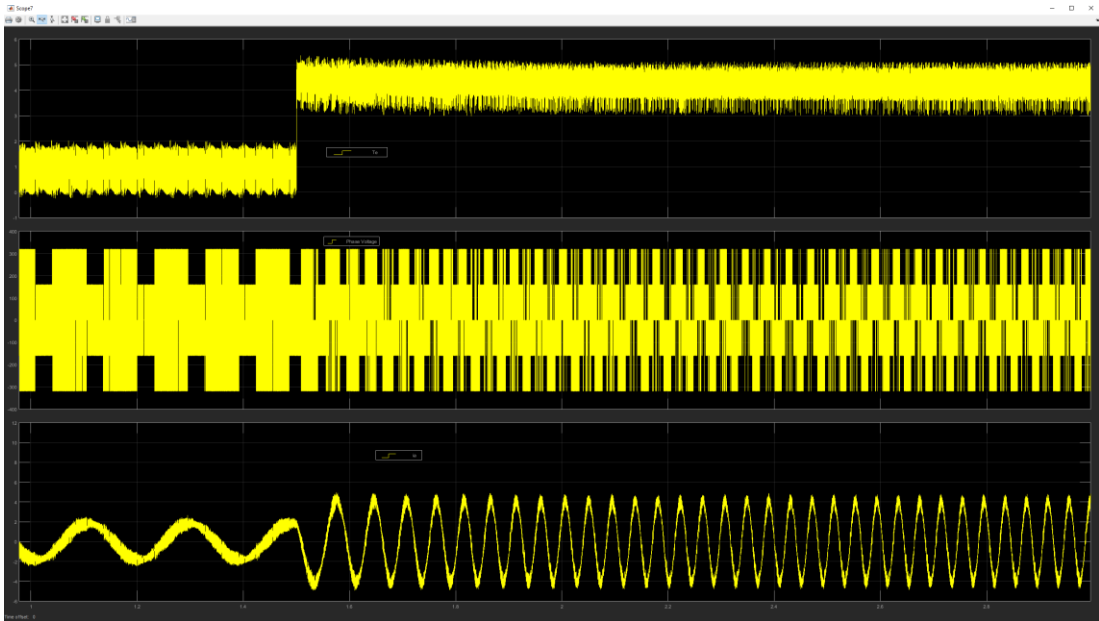


(a)

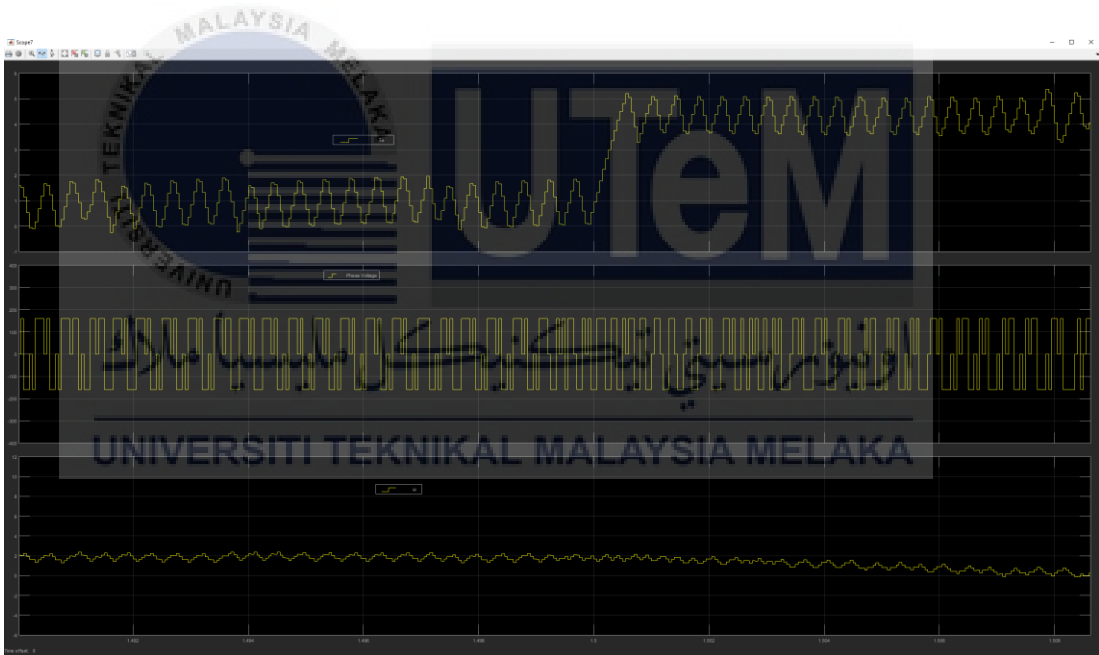


(b)

Figure 25: Waveform of Torque, Phase Voltage and Phase current for a Step Change of Reference Torque in DTC with Non-Optimized Switching Strategy at Low-Speed Operation (a) General View (b) Zoom-in Version

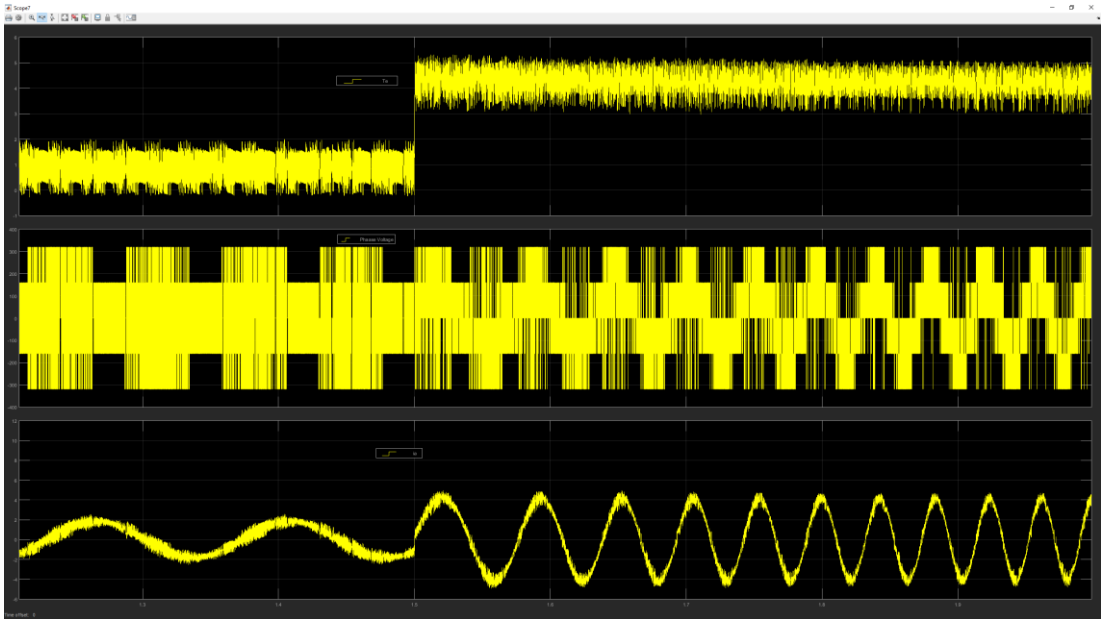


(a)

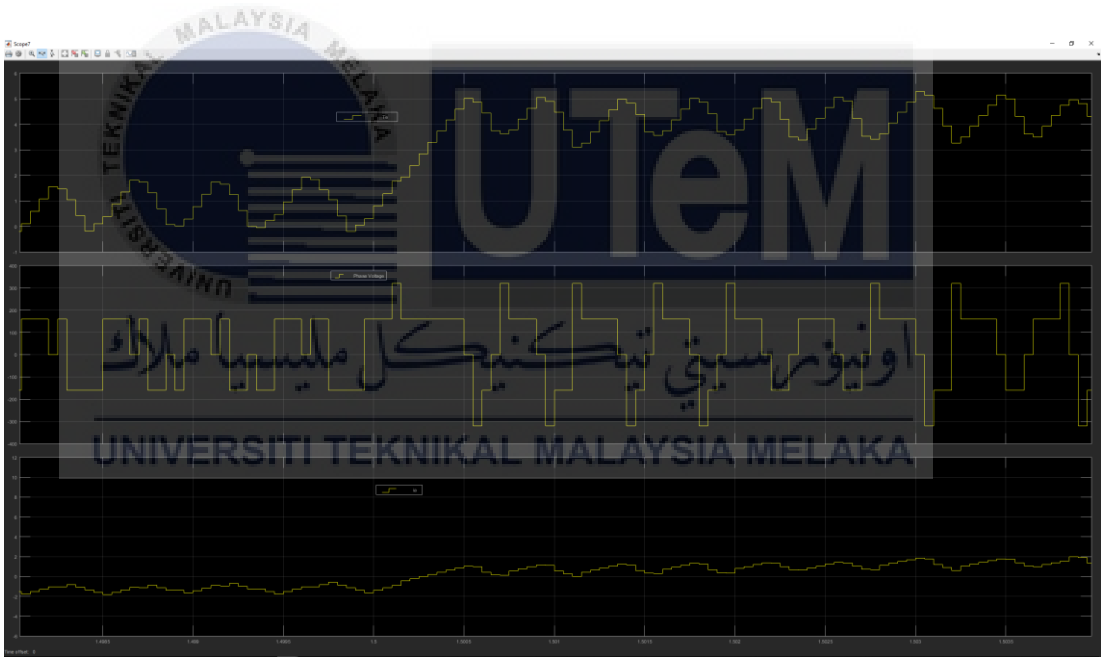


(b)

Figure 26: Waveform of Torque, Phase Voltage and Phase current for a Step Change of Reference Torque in DTC with Non-Optimized Switching Strategy at Medium-Speed Operation (a) General View (b) Zoom-in Version

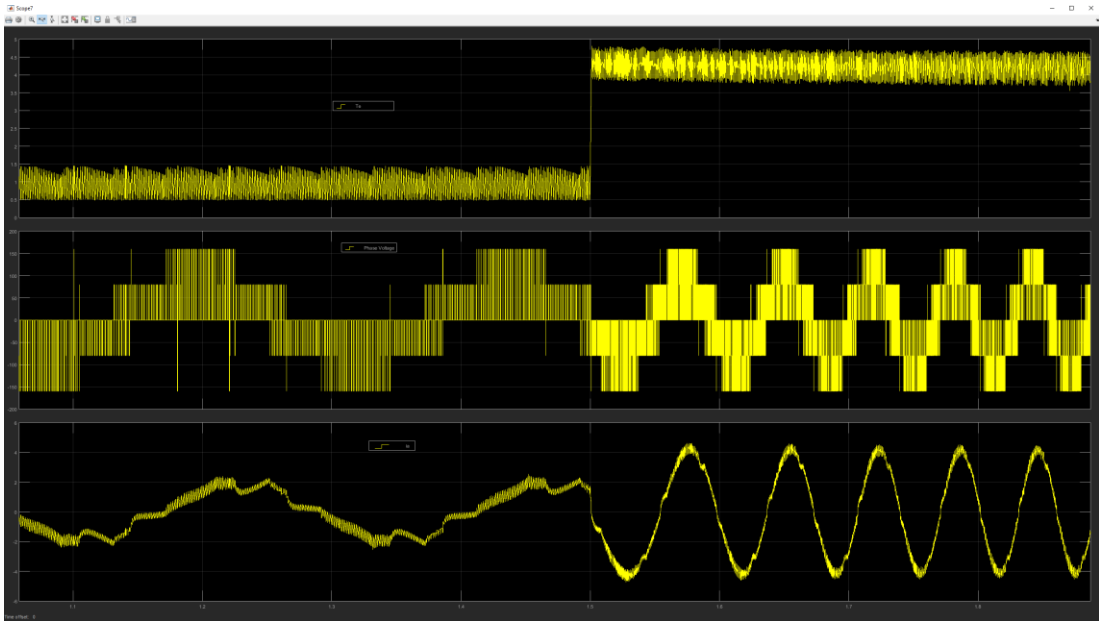


(a)

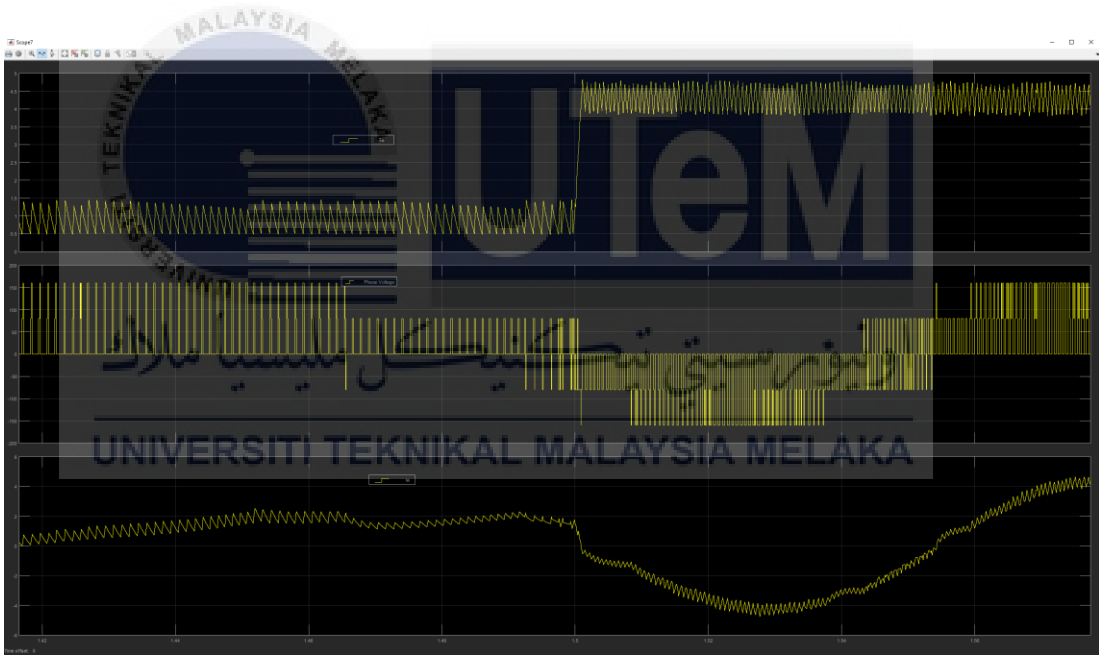


(b)

Figure 27: Waveform of Torque, Phase Voltage and Phase current for a Step Change of Reference Torque in DTC with Non-Optimized Switching Strategy at High-Speed Operation (a) General View (b) Zoom-in Version

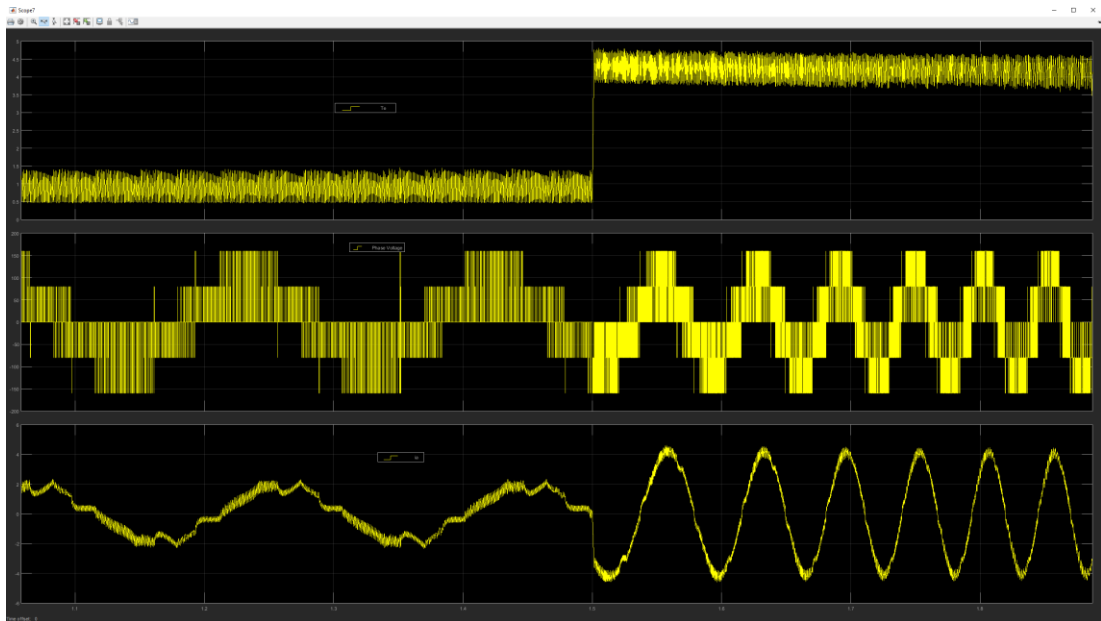


(a)

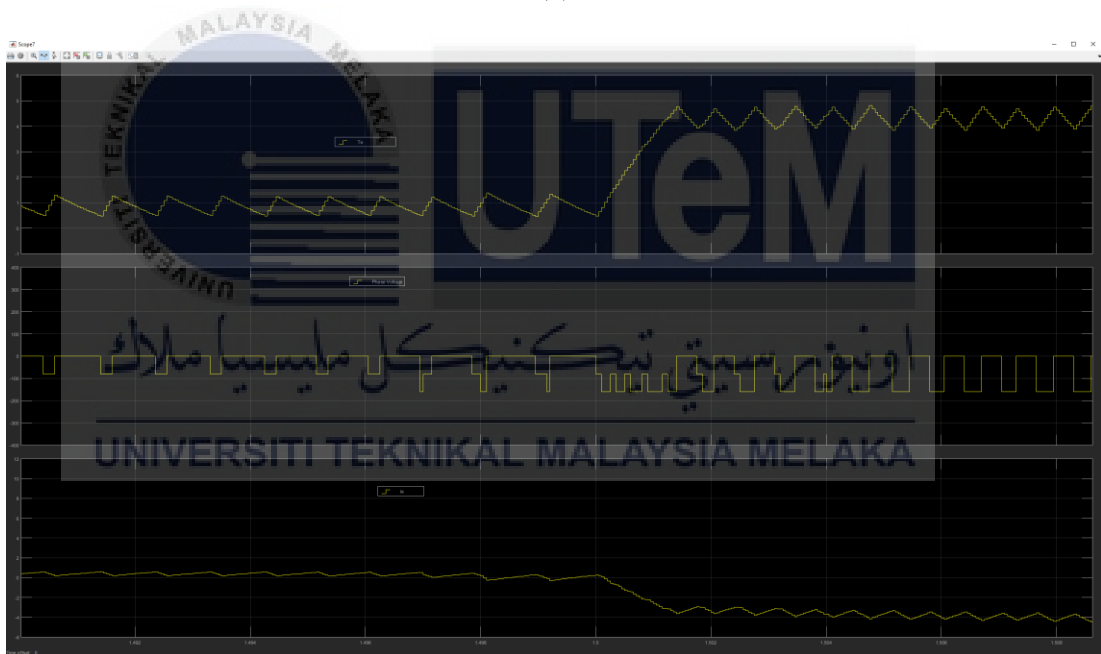


(b)

Figure 28: Waveform of Torque, Phase Voltage and Phase current for a Step Change of Reference Torque in DTC with Optimized Switching Strategy at Low-Speed Operation (a) General View (b) Zoom-in Version

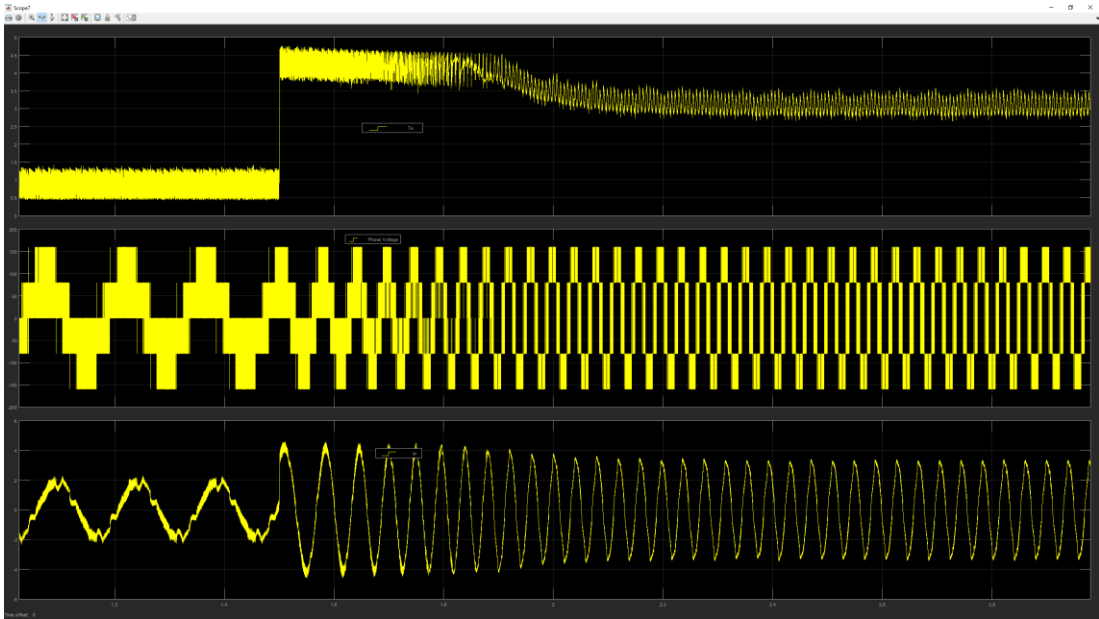


(a)

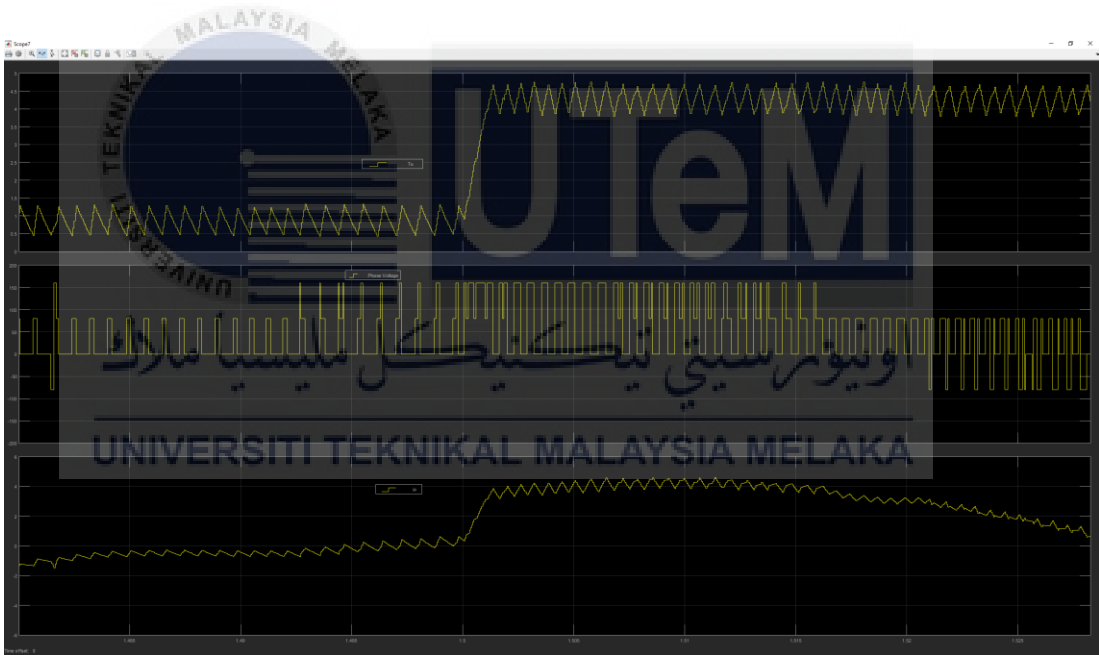


(b)

Figure 29: Waveform of Torque, Phase Voltage and Phase current for a Step Change of Reference Torque in DTC with Optimized Switching Strategy at Medium-Speed Operation (a) General View (b) Zoom-in Version



(a)

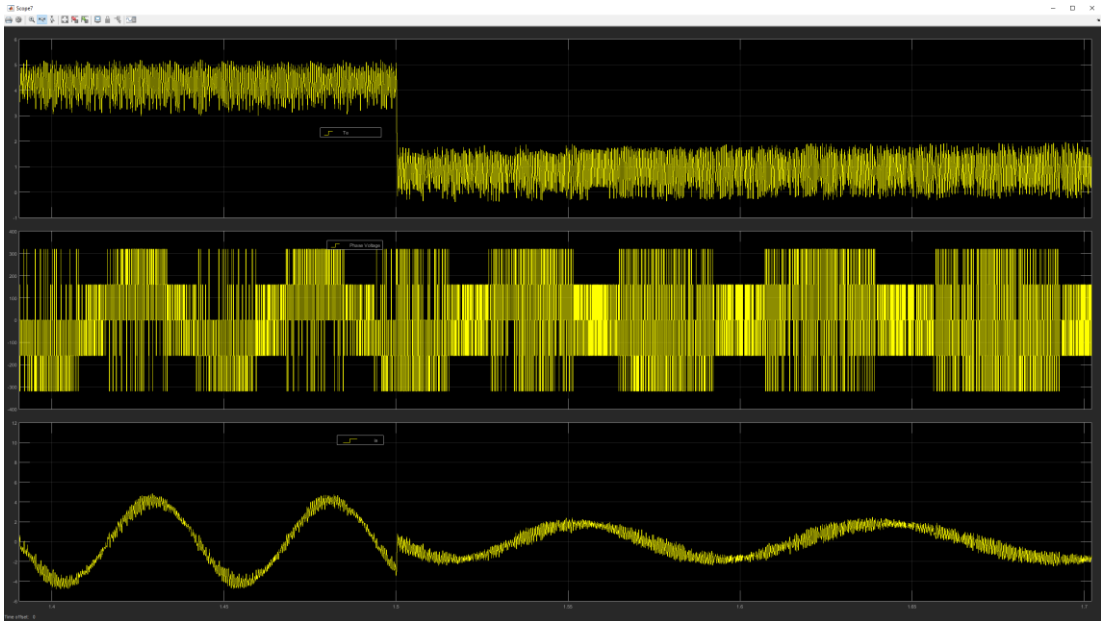


(b)

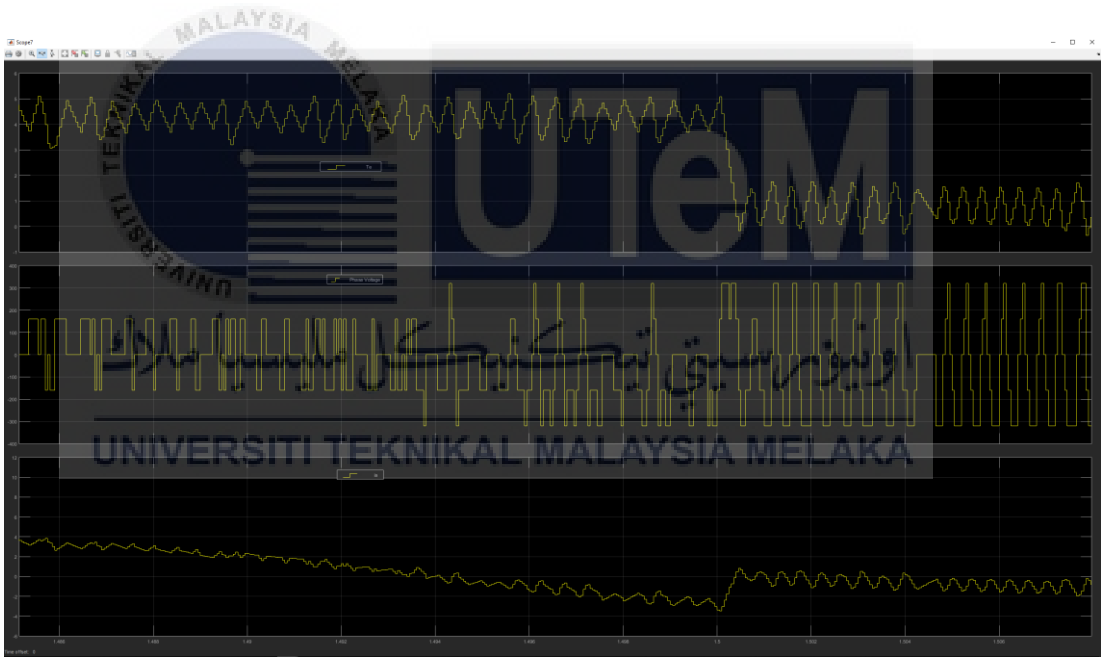
Figure 30: Waveform of Torque, Phase Voltage and Phase current for a Step Change of Reference Torque in DTC with Optimized Switching Strategy at High-Speed Operation (a) General View (b) Zoom-in Version

Besides, the optimized method can also be applying on the step reduction of reference torque. The result of the effectiveness of this method will be the same as the step change but in the reverse manners. The Figure 31 to Figure 33 shows the waveform of torque, phase voltage and phase current for a step reduction of reference torque in DTC with non-optimized switching strategy at low, medium and high speed. From Figure 34 to Figure 36 shows the waveforms torque, phase voltage and phase current for the step reduction of reference torque of the simulation using the DTC with optimized switching strategy.



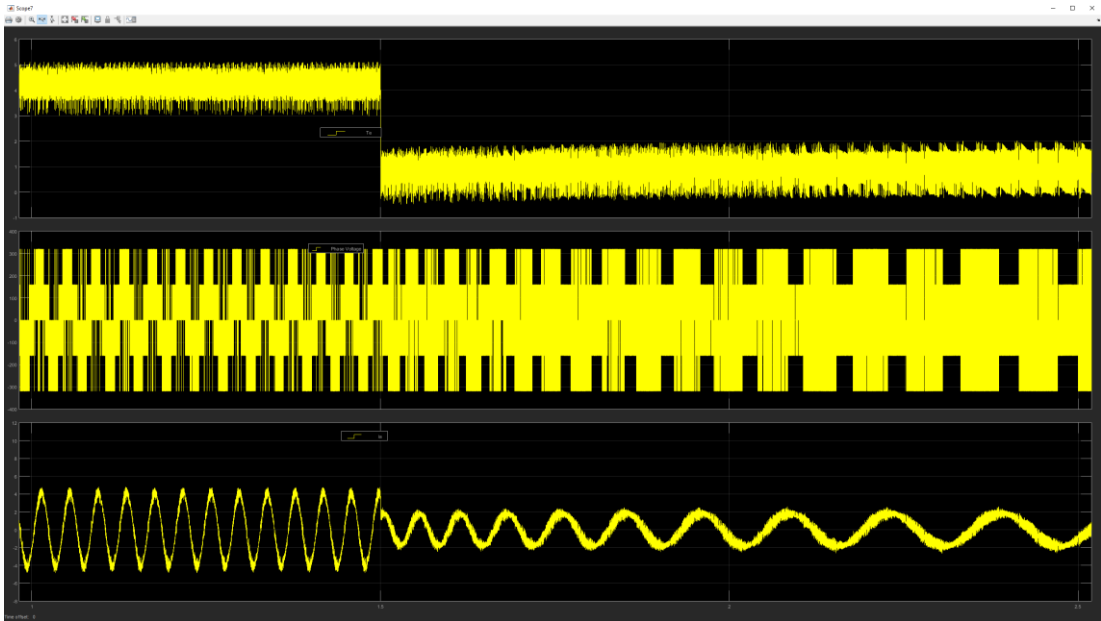


(a)

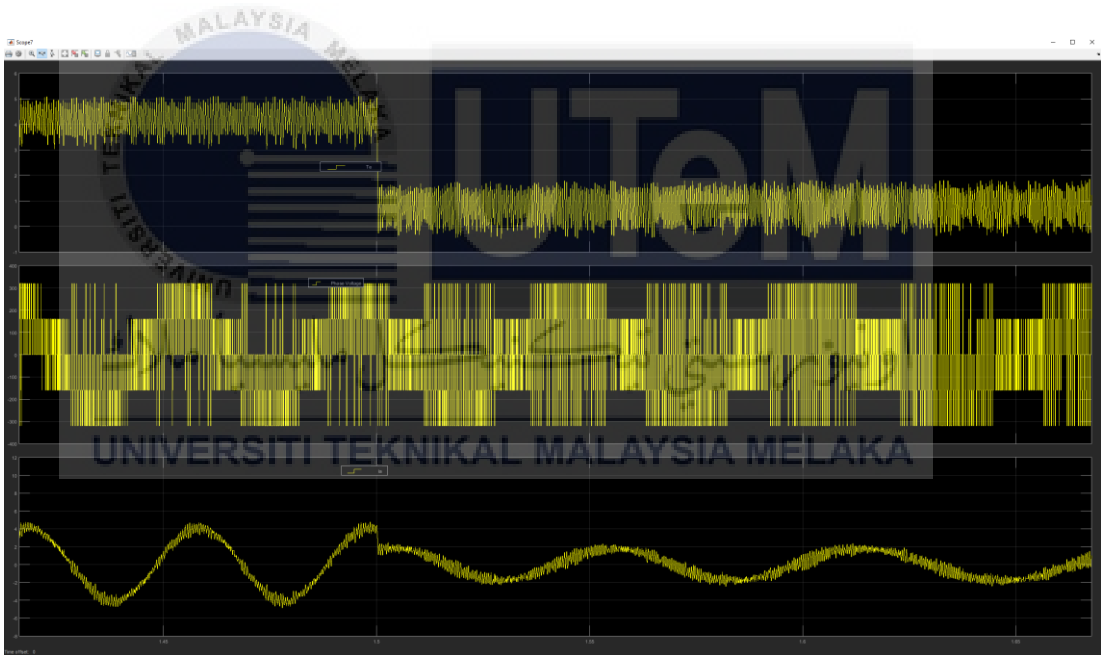


(b)

Figure 31: Waveform of Torque, Phase Voltage and Phase current for a Step Reduction of Reference Torque in DTC with Non-Optimized Switching Strategy at Low-Speed Operation (a) General View (b) Zoom-in Version

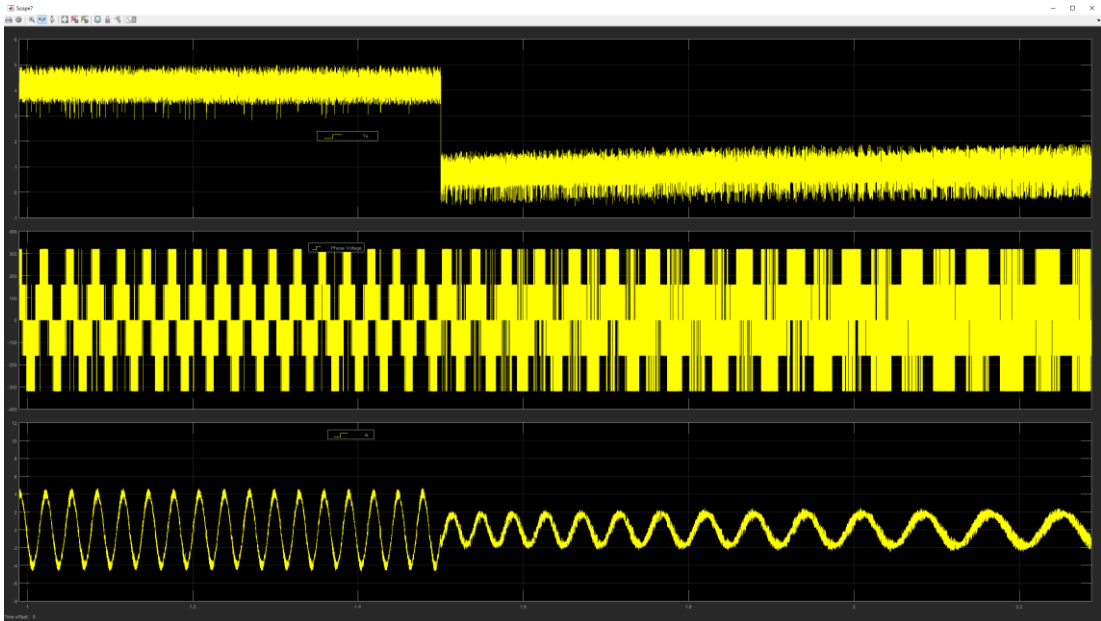


(a)

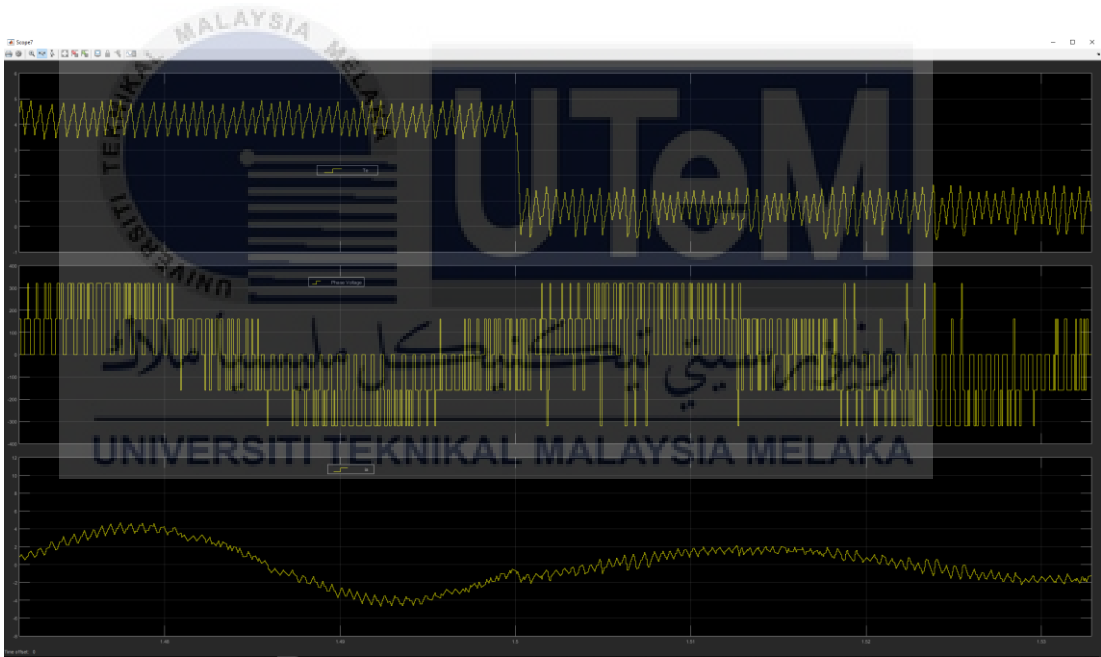


(b)

Figure 32: Waveform of Torque, Phase Voltage and Phase current for a Step Reduction of Reference Torque in DTC with Non-Optimized Switching Strategy at Medium-Speed Operation (a) General View (b) Zoom-in Version

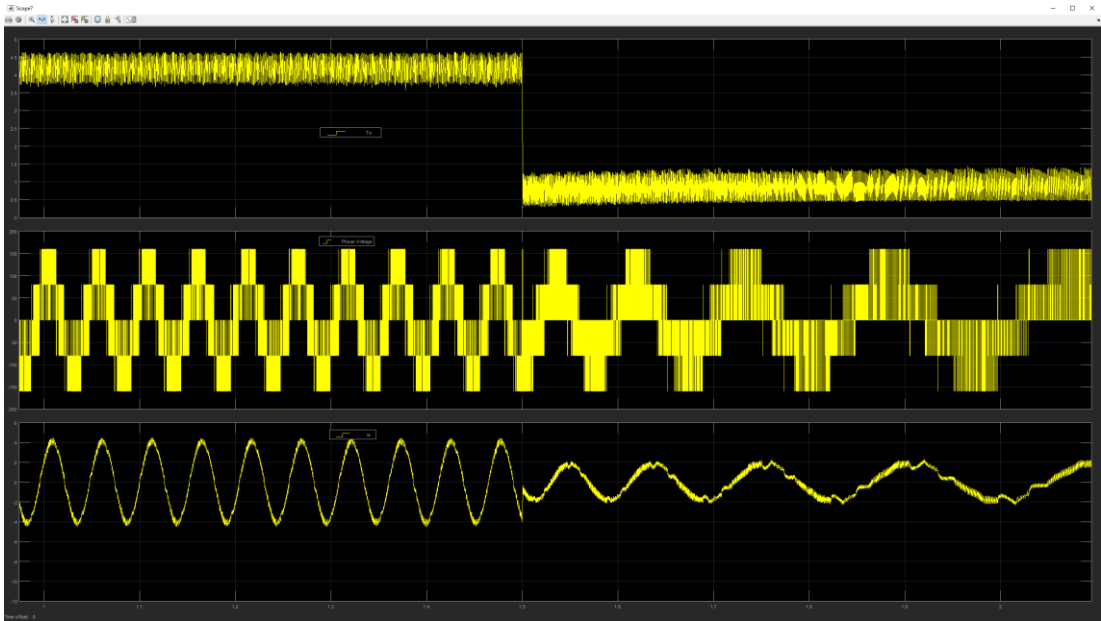


(a)

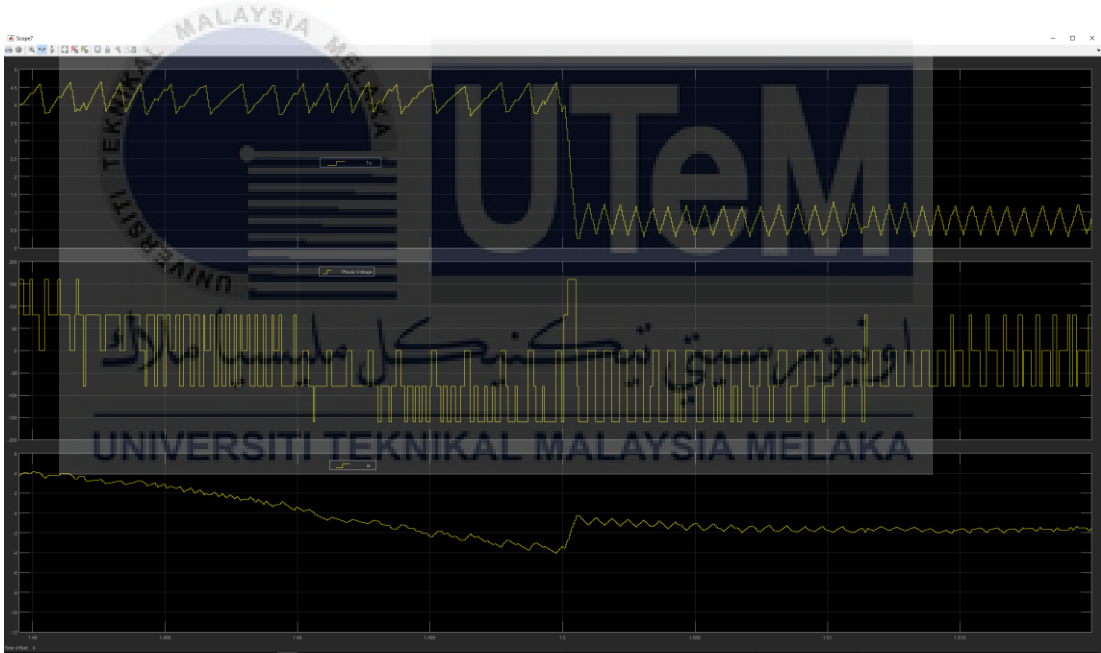


(b)

Figure 33: Waveform of Torque, Phase Voltage and Phase current for a Step Reduction of Reference Torque in DTC with Non-Optimized Switching Strategy at High-Speed Operation (a) General View (b) Zoom-in Version

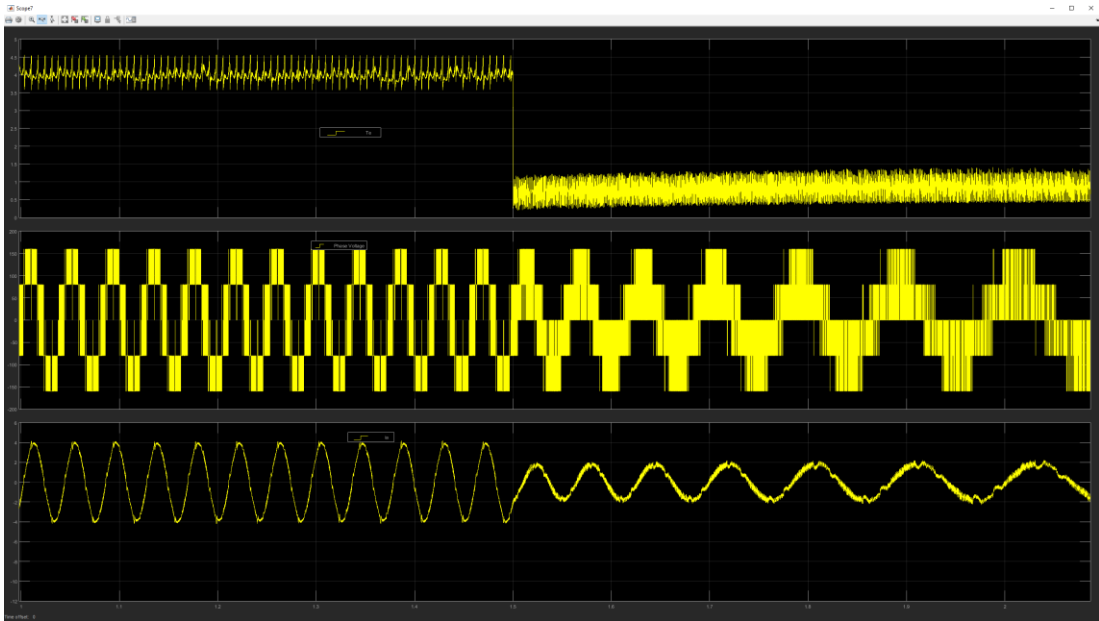


(a)

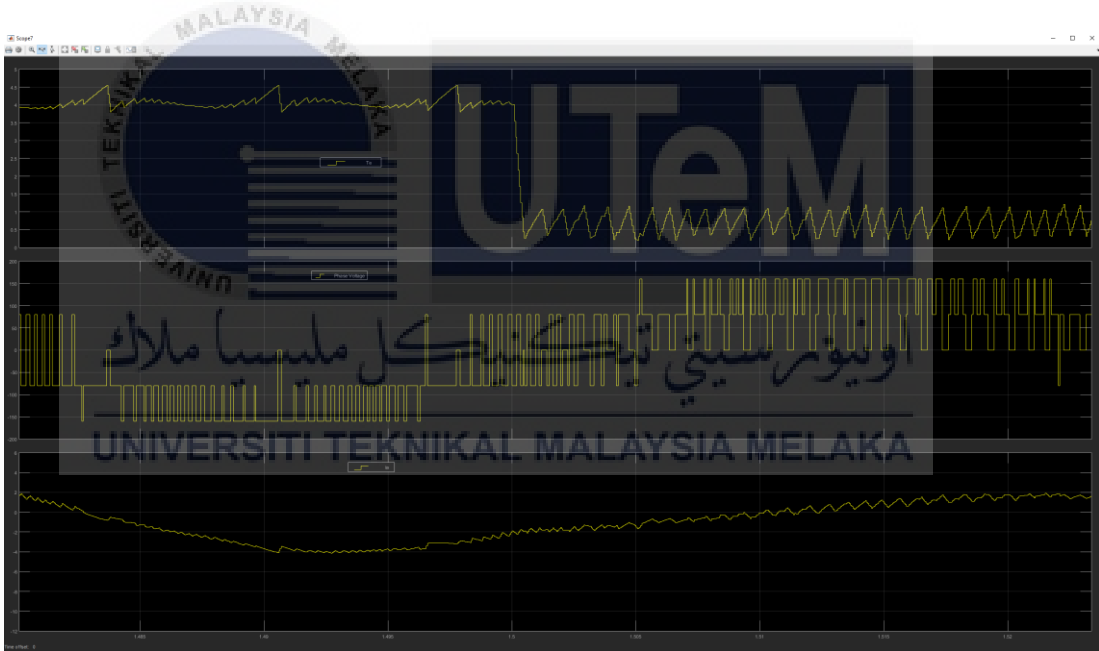


(b)

Figure 34: Waveform of Torque, Phase Voltage and Phase current for a Step Reduction of Reference Torque in DTC with Optimized Switching Strategy at Low-Speed Operation (a) General View (b) Zoom-in Version

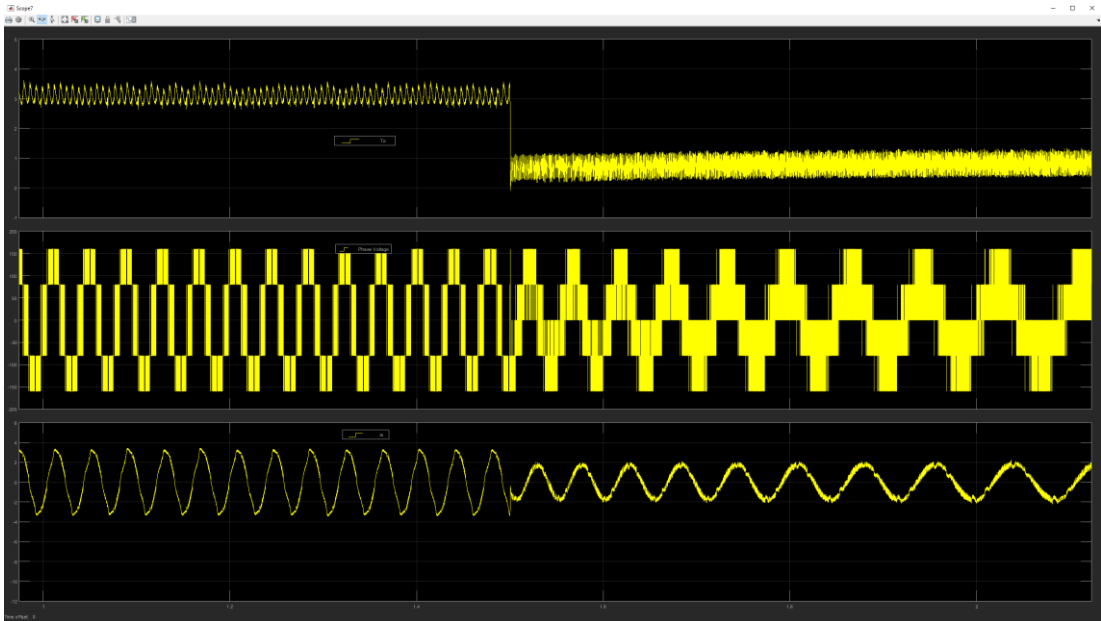


(a)

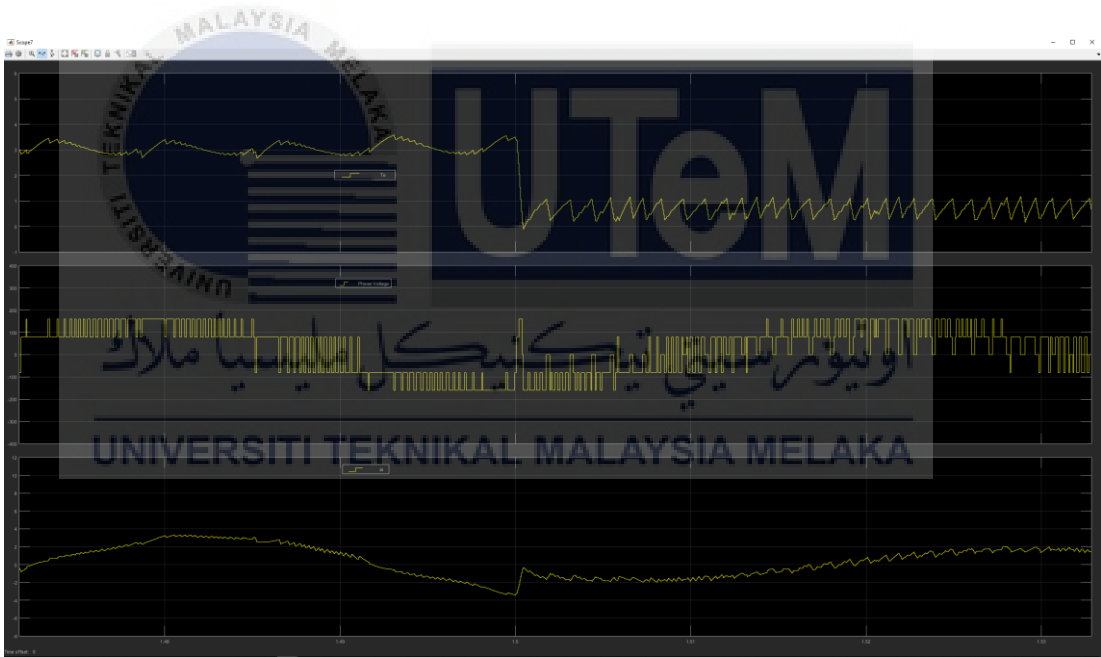


(b)

Figure 35: Waveform of Torque, Phase Voltage and Phase current for a Step Reduction of Reference Torque in DTC with Optimized Switching Strategy at Medium-Speed Operation (a) General View (b) Zoom-in Version



(a)



(b)

Figure 36: Waveform of Torque, Phase Voltage and Phase current for a Step Reduction of Reference Torque in DTC with Optimized Switching Strategy at High-Speed Operation (a) General View (b) Zoom-in Version

CHAPTER 5

Conclusion and Recommendation

5.1 Conclusion

The overall objectives of this thesis are to reduce torque ripple and switching frequency for open-end winding induction machines. With the carried experiments or simulations, it shown that the more the number of voltage vector offered, the better the effect in reduction of torque ripple and switching frequency.

In achieving these improvements, this research has made some contributions as follow:

- Retaining the simplicity of the conventional DTC structure to eliminate the use of speed sensors.
- Torque ripple and switching frequency been reduced with the selection of appropriate voltage vectors.
- The proposed optimal switching strategy select the voltage vector that shows the most tangential to the flux vector and the longest amplitude during torque dynamic condition for producing the fastest torque dynamic response.

These improvements of the proposed methods are tested with simulation and experimental results. It has shown that the proposed method successfully in reducing

the torque ripple and the switching frequency by selecting the suitable voltage vector according the sector and the tangential to the flux vector.

5.2 Recommendations

Some recommendations for future work to improve further the DTC performances,

- Add in Fuzzy Logic Control (FLC) in to the design to achieve a more robust in control. The suitable voltage vector in the proposed method was depending on the comparison between the switching for torque hysteresis controller and flux hysteresis controller, by choosing the appropriate threshold value. By applying FLC, the selection of suitable voltage vector can be simplified.
- Replacing the hysteresis controller with constant frequency torque controller to provide a constant switching frequency. As using hysteresis will lead to variation of switching frequency.

References

Baiju, M.R., Mohapatra, K. K., Kanchan, R. S. and Gopakumar, K., 2004. A dual two-level inverter scheme with common mode voltage elimination for an induction motor drive. *IEEE Transactions on Power Electronic*, 19, pp.794-805.

Beerten, J., Verwekken, J. and Driesen, J., 2010. Predictive Direct Torque Control for Flux and Torque Ripple Reduction. *IEEE Transactions on Industrial Electronics*, 57, pp. 404-412.

Bird, I. G. and Zelaya De La Parra, H., 1996. Practical evaluation of two stator flux estimation techniques for high performance direct torque control. *Sixth International Conference on Power Electronics and Variable Speed Drives*, pp.465-470.

Blaschke, F. 1972. The principle of field orientation as applied to the new Transvektor closed-loop control system for rotating field machines. 34, 217-220.

Bo, Z., Qiongquan, G., Qiankun, C. and Shutian, Z., 2014. Research on a sensorless SVM-DTC strategy for induction motors based on modified stator model. *2014 IEEE 9th Conference on Industrial Electronics and Applications (ICIEA)*, pp. 1724-1729.

Brando, G., Dannier, A., Pizzo, A. D., Rizzo, R. and Spina, I., 2015. Generalised look-up table concept for direct torque control in induction drives with multilevel inverters. *IET Electric Power Applications*, 9, pp.556-567.

Casadei, D., Grandi, G., Serra, G. and Tani, A., 1994. Effect of flux and torque hysteresis band amplitude in direct torque control of induction motor. In Conf. Rec., IEEE-IECON'94, pp. 299-304.

Casadei, D., Grandi, G., Serra, G. and Tani, A., 1994. Switching strategies in direct torque control of induction machine. In Conf. Rec. International Conf. on Electrical Machines, Paris, France, pp. 204-209.

Casadei, D., Serra, G., Stefani, A., Tani, A. and Zarri, L., 2007. DTC Drives for Wide Speed Range Applications Using a Robust Flux-Weakening Algorithm. IEEE Transactions on Industrial Electronics, 54, pp.2451-2461.

Casadei, D., Serra, G., Stefani, A., Tani, A. 1997. Analytical investigation of torque and flux ripple in DTC schemes for induction motors. 23rd International Conference on Industrial Electronics, Control and Instrumentation IECON 97, vol.2, pp.552-556.

Casadei, D., Serra, G., Stefani, A., Tani, A. 1998. Improvement of direct torque control performance by using a discrete SVM technique. Power Electronic Specialist Conference, 1998. PESC 98 Record. 29th Annual IEEE, vol.2, pp.997-1003.

Celanovic, N, and Boroyevich, D. 2001. A fast space-vector modulation algorithm for multilevel three-phase converters. Industry Applications, IEEE Transactions on, 37, pp.637-641.

Corzine, K. A., Sudhoff, S. D. and Whitcomb, C. A., 1999. Performance characteristics of cascaded two-level converter. IEEE Transactions on Energy Conversion, 14, pp.433-439.

D. Swierczynski, M. Z. 2004. Universal Structure of Direct Torque Control for AC Motor Drives. *Przeegląd Elektrotechniczny*, pp.489-492.

Gracia, G. O., Stephan, R. M. and Watanabe, E. H., 1994. Comparing the indirect field-oriented control with a scalar method, *IEEE Transactions on Industrial Electronics*, 41, pp.201-207.

Gupta, K. K., Ranjan, A., Bhatnagar, P., Sahu, L. K. and Jain, S., 2016. Multilevel Inverter Topologies with Reduced Device Count: A Review. *IEEE Transactions on Power Electronics*, 31, pp.135-151.

Habetler, T. G., Profumo, F., Pastorelli, M. and Tolbert, L. M., 1992. Direct Torque Control of Induction Machines Using Space Vector Modulation. *Industry Applications, IEEE Transactions on*. 28, pp.1045-1053.

Haoran, Z., Von Jouanne, A., Shaoan, D., Wallace, A. K. and Fei, W., 2000. Multilevel inverter modulation schemes to eliminate common-mode voltages. *Industry Applications, IEEE Transactions on*, 36, pp.1645-1653.

Hu, J. and Wu, B., 1997. New integration algorithms for estimating motor flux over a wide speed range. 28th Annual IEEE Power Electronic Specialists Conference, PESC '97 Record, vol.2, pp.1075-1081.

Idris, N. R. N. and Yatim, A. H. M., 2000. An improved stator flux estimation in steady state operation for direct torque control of induction machines. *Industry Applications Conference, Conference Record of the 2000 IEEE*, vol.3, pp.1353-1359.

Idris, N. R. N. and Yatim, A. H. M., 2004. Direct torque control of induction machines with constant switching frequency and reduced torque ripple. *Industrial Electronics, IEEE Transactions on*, 51, pp.758-767.

Jae Hyeong, S., Chang Ho, C. and Dong-Seok, H., 2001. A new simplified space-vector PWM method for three-level inverters. *Power Electronics, IEEE Transactions on*, 16, pp.545-550.

Jidin, A., Idris, N. R. N., Yatim, A. H. M., Sutikno, T. and Elbuluk, M. E., 2011. Extending switching frequency for torque ripple reduction utilizing a constant frequency torque controller in DTC of induction motors. *Journal of Power Electronics*, 11, pp.148-155.

Jidin, A., Idris, N. R. N., Yatim, A. H. M., 2008. A simple overmodulation strategy in DTC-hysteresis based induction machine drives. *IEEE 2nd International on Power and Energy Conference, PECon 2008*, pp.722-725.

Jun-Koo, K. and Seung-Ki, S., 1999. New direct torque control of induction motor for minimum torque ripple and constant switching frequency. *Industry Applications, IEEE Transactions on*, 35, pp.1076-1082.

Kang, J. W. and Sul, S. K., 2001. Analysis and prediction of inverter switching frequency in direct torque control of induction machine based on hysteresis bands and machine parameters. *IEEE Transactions on Industrial Electronics*, 48, pp.545-553.

Kumar, H. R., Harish, K. and Rao, S. S., 2015. Predictive torque-controlled induction motor drive with reduced torque and flux ripple over DTC. *2015 International*

Conference on Electrical, Electronics, Signals, Communication and Optimization (EESCO), pp.1-6.

Kumar, A., Fernandes, B. G. and Chatterjee, K., 2004. DTC of open-end winding induction motor drive using space vector modulation with reduced switching frequency. 2004 IEEE 35th Annual on Power Electronic Specialists Conference, PESC, vol.2, pp.1214-1219.

Lascu, C., Boldea, I. and Blaabjerg, F., 2000. A modified direct torque control for induction motor sensorless drive. Industry Applications, IEEE Transactions on, 36, pp.122-130.

Lascu, C., Boldea, I. and Blaabjerg, F., 2004. Variable- Structure direct torque control- a class of fast and robust controllers for induction machine drives. IEEE Transactions on Industrial Electronics, 51, pp.758-792.

Malinowski, M., Gopakumar, K., Rodriguez, J., Pe, X and Rez, M. A., 2010. A Survey on Cascaded Multilevel Inverters. Industrial Electronics, IEEE Transactions on, 57, pp. 2197-2206.

Martins, C. A., Roboam, X., Meynard, T. A. and Carvalho A, S., 2002. Switching frequency imposition and ripple reduction in DRC drives by using a multilevel converter. IEEE Transactions on Power Electronics, 17, pp.286-297.

APPENDIX A

MATLAB SIMULATION BLOCK CODING

A.1 Sector Detection Block Coding

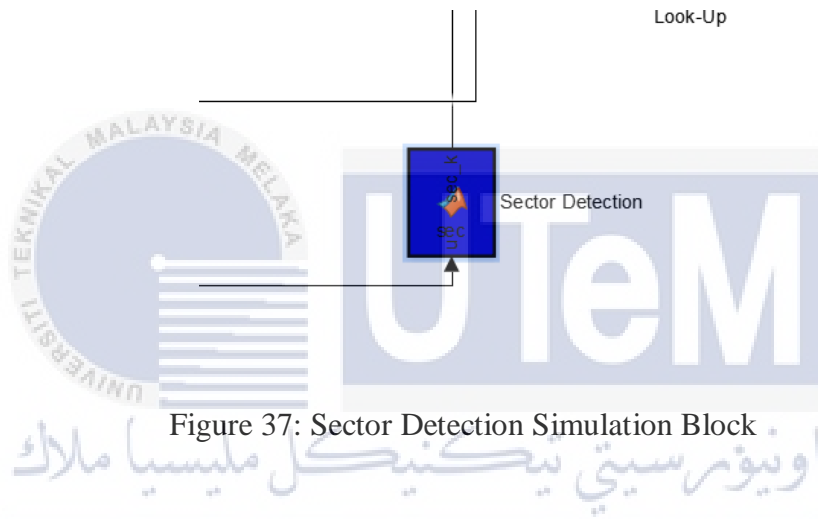


Figure 37: Sector Detection Simulation Block

```
function sec_k = sec(u)
% u[1] = angle, y[0] = sector
sector=1;
angle = u(1);
if( (angle >= -pi/6) && (angle < pi/6))
    sector = 2;
elseif ((angle >= pi/6) && (angle < pi/2))
    sector = 3;
elseif ((angle >= pi/2) && (angle < 5*pi/6))
    sector = 4;
elseif ((angle >= 5*pi/6) || (angle < -5*pi/6))
    sector = 5;
elseif ((angle >= -5*pi/6) && (angle < -pi/2))
```

```
sector = 6;  
elseif ((angle >= -pi/2) && (angle < -pi/6))  
    sector = 1;  
end  
sec_k =[sector];  
end
```



A.2 Look-up Table Coding

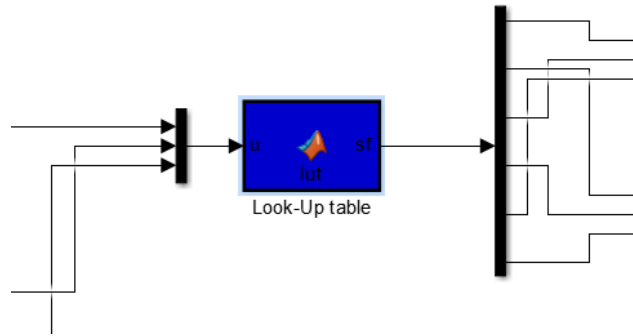


Figure 38: Look-up Table Simulation Block

```

%Standard Look-up table (LUT) proposed by Takahashi
%input: torque error status=u(1), flux error status=u(2) and sector=(3)

function sf = lut(u)
%initialization the output switching status, i.e. sa, sb and sc
sx = [0 0 0 0 0 0];

%Obtain the inputs to index the LUT
tstat = u(1);
fstat = u(2);
sec = u(3);

%Selection of vector for Sector 1
if(sec == 1)
    if(fstat == 1)
        if (tstat == 3)
            sx = [1 0 0 1 0 1];
        elseif (tstat == 2)
            sx = [0 1 0 0 1 0];
        elseif (tstat == 1)

```



```

    sx = [0 0 0 1 0 1];
elseif (tstat == 0)
    sx = [0 1 0 1 0 1];
elseif (tstat == -1)
    sx = [0 1 0 1 0 0];
elseif (tstat == -2)
    sx = [0 0 1 0 0 1];
elseif (tstat == -3)
    sx = [0 1 0 1 1 0];
end

```

```
elseif (fstat == 0)
```

```
    if (tstat == 3)
```

```
        sx = [1 0 1 0 0 1];
```

```
    elseif (tstat == 2)
```

```
        sx = [0 0 0 1 1 0];
```

```
    elseif (tstat == 1)
```

```
        sx = [1 0 1 0 0 0];
```

```
    elseif (tstat == 0)
```

```
        sx = [1 0 1 0 1 0];
```

```
    elseif (tstat == -1)
```

```
        sx = [0 0 1 0 1 0];
```

```
    elseif (tstat == -2)
```

```
        sx = [1 0 0 0 0 1];
```

```
    elseif (tstat == -3)
```

```
        sx = [0 1 1 0 1 0];
```

```
    end
```

```
end
```

```
%Selection of vector for Sector 2
```

```
elseif(sec == 2)
```

```
    if(fstat == 1)
```

```
        if (tstat == 3)
```

```
            sx = [1 0 1 0 0 1];
```

```

elseif (tstat == 2)
    sx = [0 1 1 0 0 0];
elseif (tstat == 1)
    sx = [1 0 1 0 0 0];
elseif (tstat == 0)
    sx = [1 0 1 0 1 0];
elseif (tstat == -1)
    sx = [1 0 0 0 1 0];
elseif (tstat == -2)
    sx = [1 0 0 0 0 1];
elseif (tstat == -3)
    sx = [1 0 0 1 1 0];
end

```

```

elseif (fstat == 0)
    if (tstat == 3)
        sx = [0 1 1 0 0 1];
    elseif (tstat == 2)
        sx = [0 1 0 0 1 0];
    elseif (tstat == 1)
        sx = [0 1 0 0 0 1];
    elseif (tstat == 0)
        sx = [0 1 0 1 0 1];
    elseif (tstat == -1)
        sx = [0 1 0 1 0 0];
    elseif (tstat == -2)
        sx = [1 0 0 1 0 0];
    elseif (tstat == -3)
        sx = [0 1 0 1 1 0];
    end
end

```

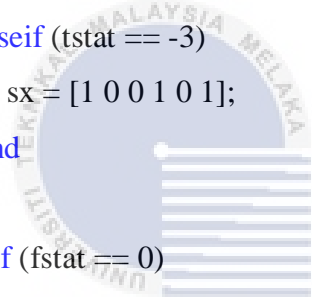
%Selection of vector for Sector 3

```
elseif(sec == 3)
```

```

if(fstat == 1)
  if (tstat == 3)
    sx = [0 1 1 0 0 1];
  elseif (tstat == 2)
    sx = [0 0 1 0 0 1];
  elseif (tstat == 1)
    sx = [0 1 0 0 0 1];
  elseif (tstat == 0)
    sx = [0 1 0 1 0 1];
  elseif (tstat == -1)
    sx = [0 0 0 1 0 1];
  elseif (tstat == -2)
    sx = [1 0 0 1 0 0];
  elseif (tstat == -3)
    sx = [1 0 0 1 0 1];
end
elseif (fstat == 0)
  if (tstat == 3)
    sx = [0 1 1 0 1 0];
  elseif (tstat == 2)
    sx = [0 1 1 0 0 0];
  elseif (tstat == 1)
    sx = [0 0 1 0 1 0];
  elseif (tstat == 0)
    sx = [1 0 1 0 1 0];
  elseif (tstat == -1)
    sx = [1 0 0 0 1 0];
  elseif (tstat == -2)
    sx = [0 0 0 1 1 0];
  elseif (tstat == -3)
    sx = [1 0 0 1 1 0];
  end
end
end

```



اونيورسيتي تيكنيكل ملسيا ملاك
 UNIVERSITI TEKNIKAL MALAYSIA MELAKA

%Selection of vector for Sector 4

```
elseif(sec == 4)
    if(fstat == 1)
        if (tstat == 3)
            sx = [0 1 1 0 1 0];
        elseif (tstat == 2)
            sx = [1 0 0 0 0 1];
        elseif (tstat == 1)
            sx = [0 0 1 0 1 0];
        elseif (tstat == 0)
            sx = [1 0 1 0 1 0];
        elseif (tstat == -1)
            sx = [1 0 1 0 0 0];
        elseif (tstat == -2)
            sx = [0 0 0 1 1 0];
        elseif (tstat == -3)
            sx = [1 0 1 0 0 1];
        end
    elseif (fstat == 0)
        if (tstat == 3)
            sx = [0 1 0 1 1 0];
        elseif (tstat == 2)
            sx = [0 0 1 0 0 1];
        elseif (tstat == 1)
            sx = [0 1 0 1 0 0];
        elseif (tstat == 0)
            sx = [0 1 0 1 0 1];
        elseif (tstat == -1)
            sx = [0 0 0 1 0 1];
        elseif (tstat == -2)
            sx = [0 1 0 0 1 0];
        elseif (tstat == -3)
            sx = [1 0 0 1 0 1];
```



```

end
end
%Selection of vector for Sector 5

```

```

elseif(sec == 5)
    if(fstat == 1)
        if (tstat == 3)
            sx = [0 1 0 1 1 0];
        elseif (tstat == 2)
            sx = [1 0 0 1 0 0];
        elseif (tstat == 1)
            sx = [0 1 0 1 0 0];
        elseif (tstat == 0)
            sx = [0 1 0 1 0 1];
        elseif (tstat == -1)
            sx = [0 1 0 0 0 1];
        elseif (tstat == -2)
            sx = [0 1 0 0 1 0];
        elseif (tstat == -3)
            sx = [0 1 1 0 0 1];
        end
    end

```

```

elseif (fstat == 0)
    if (tstat == 3)
        sx = [1 0 0 1 1 0];
    elseif (tstat == 2)
        sx = [1 0 0 0 0 1];
    elseif (tstat == 1)
        sx = [1 0 0 0 1 0];
    elseif (tstat == 0)
        sx = [1 0 1 0 1 0];
    elseif (tstat == -1)
        sx = [1 0 1 0 0 0];
    elseif (tstat == -2)
        sx = [0 1 1 0 0 0];
    end

```



اونیورسیتی تکنیکل ملیسیا ملاک
 UNIVERSITI TEKNIKAL MALAYSIA MELAKA

```

elseif (tstat == -3)
    sx = [1 0 1 0 0 1];
end
end

```

%Selection of vector for Sector 6

```

elseif(sec == 6)
    if(fstat == 1)
        if (tstat == 3)
            sx = [1 0 0 1 1 0];
        elseif (tstat == 2)
            sx = [0 0 0 1 1 0];
        elseif (tstat == 1)
            sx = [1 0 0 0 1 0];
        elseif (tstat == 0)
            sx = [1 0 1 0 1 0];
        elseif (tstat == -1)
            sx = [0 0 1 0 1 0];
        elseif (tstat == -2)
            sx = [0 1 1 0 0 0];
        elseif (tstat == -3)
            sx = [0 1 1 0 1 0];
        end
    end

```

```

elseif (fstat == 0)
    if (tstat == 3)
        sx = [1 0 0 1 0 1];
    elseif (tstat == 2)
        sx = [1 0 0 1 0 0];
    elseif (tstat == 1)
        sx = [0 0 0 1 0 1];
    elseif (tstat == 0)
        sx = [0 1 0 1 0 1];
    elseif (tstat == -1)
        sx = [0 1 0 0 0 1];
    end

```



UNIVERSITI TEKNIKAL MALAYSIA MELAKA
 اونیورسیتی تکنیکل ملیسیا ملاک

```
elseif (tstat == -2)
    sx = [0 0 1 0 0 1];
elseif (tstat == -3)
    sx = [0 1 1 0 0 1];
end
end
end

%output switching status, i.e. sa, sb and sc
sf = sx;
end
```



A.3 Induction Motor Simulation Block Parameters

% Induction machine parameters

$R_s = 6.1$; % Stator resistance

$R_r = 6.2298$; % Rotor resistance

$L_s = 0.47979$; % Stator self inductance

$L_r = 0.47979$; % Rotor self inductance

$L_m = 0.4634$; % Mutual inductance

$P = 1$; % number of pole pairs

$J = 0.01$; % moment of inertia

$B = 0$; % viscous friction

$L_{ls} = L_s - L_m$; % Stator leakage inductance

$L_{lr} = L_r - L_m$; % Rotor leakage inductance

% Control system parameters

$HBT = 0.45$; % Torque hysteresis bandwidth

$HBF = 0.8 * 0.01$; % Flux hysteresis bandwidth

$f_{ref} = 0.8$; % Reference flux = 0.8

$DT = 50e-6$; % sampling period

$V_{dc} = 240$; % DC voltage

APPENDIX B

MATLAB SIMULATION BLOCK

B.1 Induction Motor Simulation Block

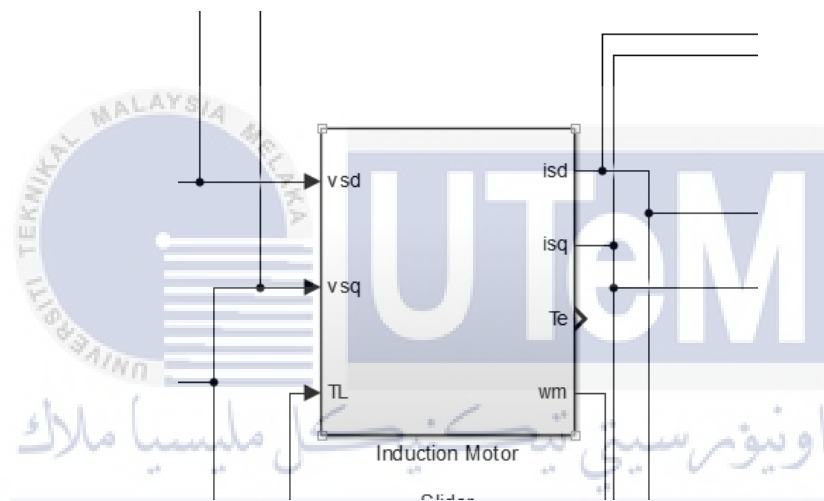


Figure 39: Induction Motor Simulation Block

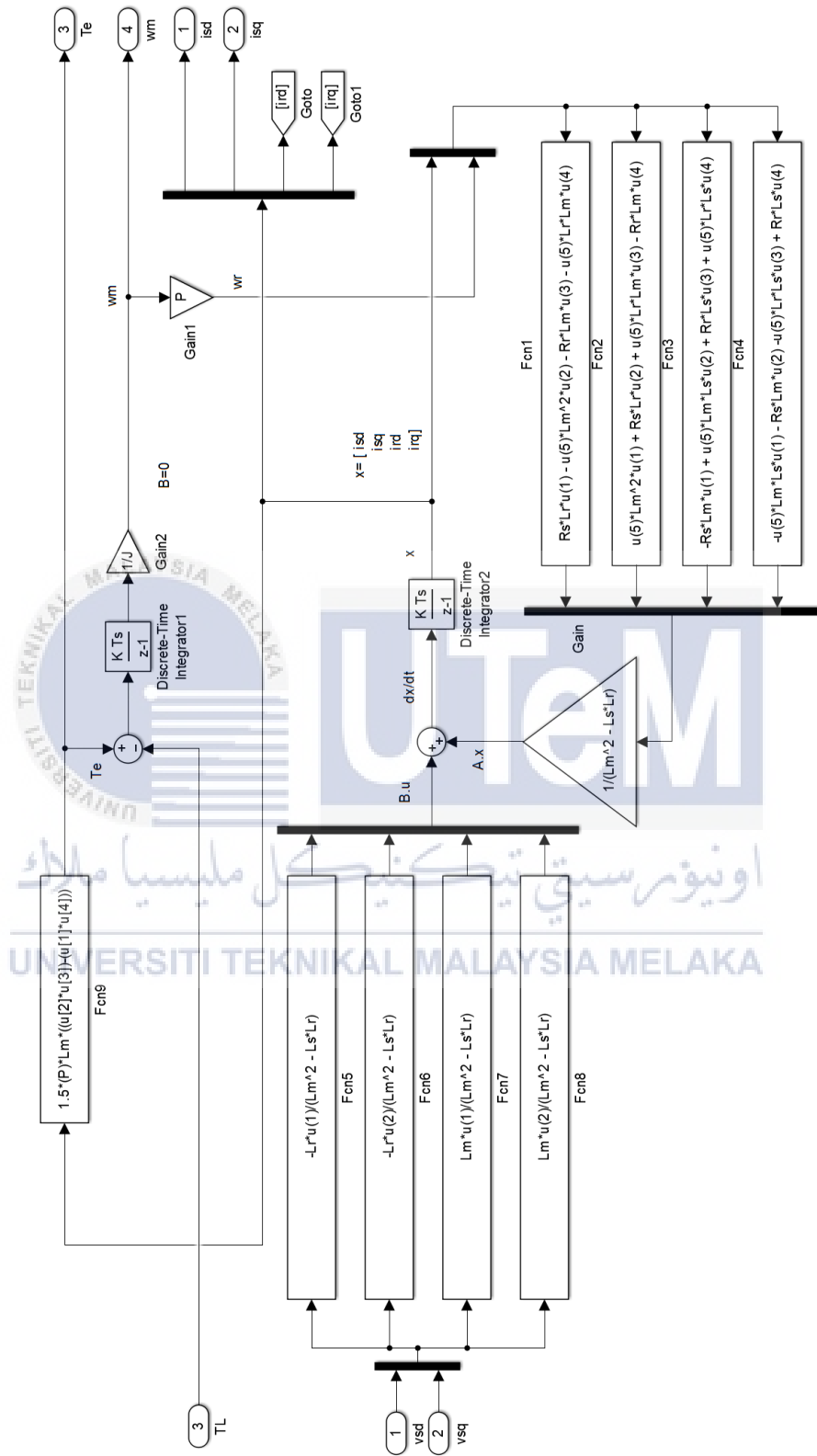


Figure 40: Interior of Induction Motor Simulation Block

B.2 Dual-Voltage Source Inverter Simulation Block

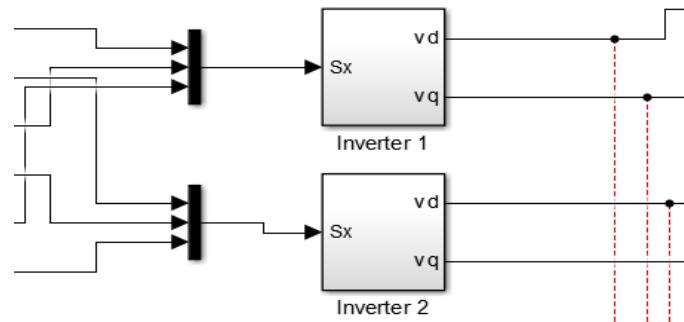


Figure 41: Dual Voltage Source Inverter Simulation Block

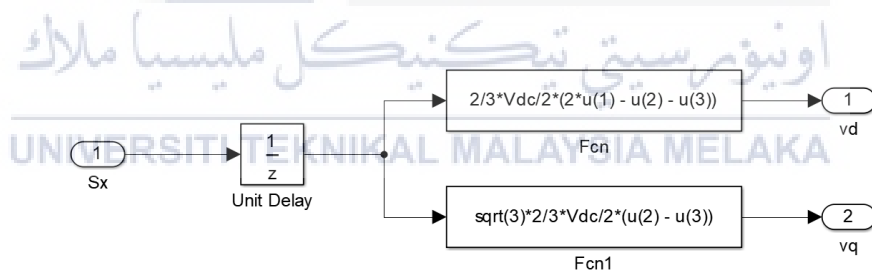


Figure 42: Interior of Dual Voltage Source Inverter Simulation Block

B.3 Torque and Flux Estimator Simulation Block

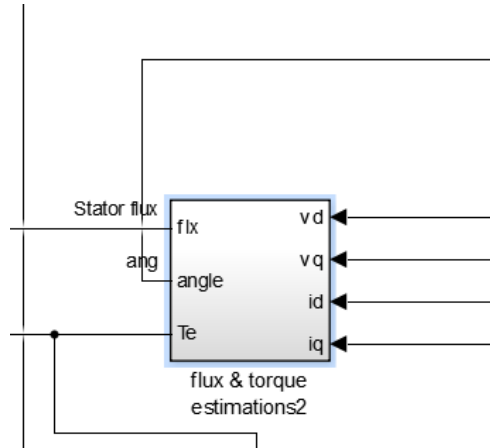


Figure 43: Torque and Flux Estimator Simulation Block

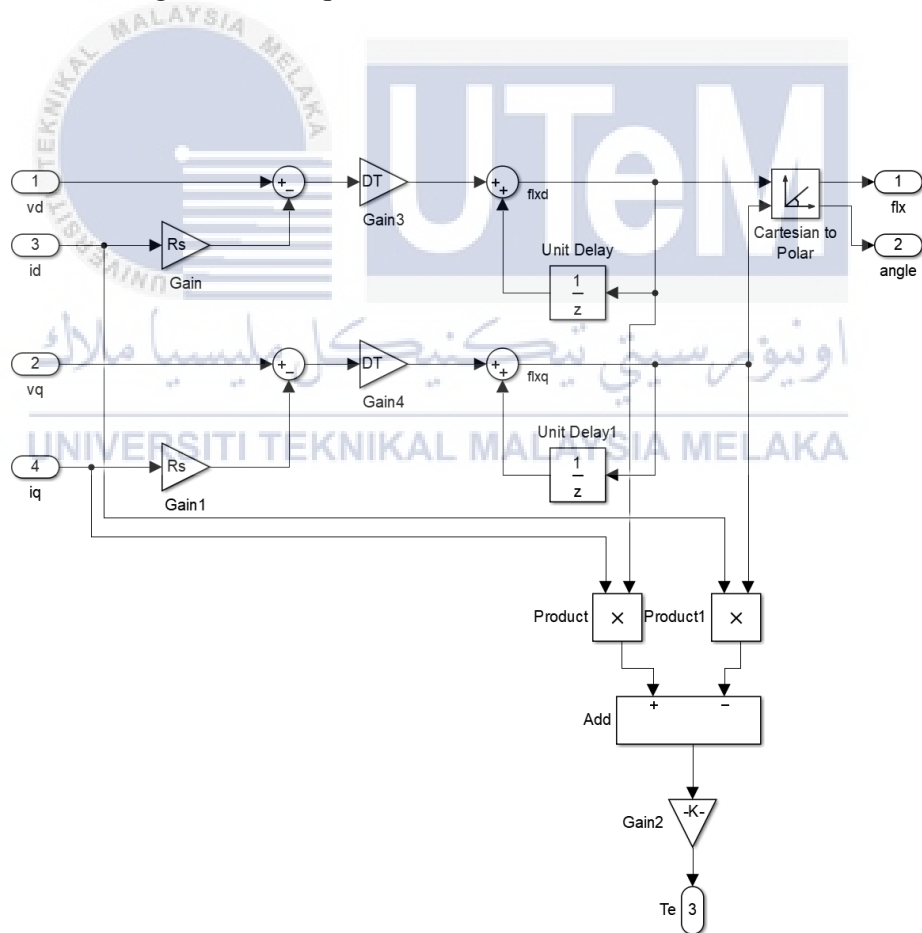


Figure 44:Interior of Torque and Flux Estimator Simulation Block